DOE/MC/23075-3151

FOSSIL ENERGY

MEASUREMENT AND MODELING OF ADVANCED COAL CONVERSION PROCESSES

23rd Quarterly Report #523043
April 1, 1992 to June 30, 1992

By
Peter R. Solomon
Michael A. Serio
David G. Hamblen
L. Douglas Smoot
B. Scott Brewster

Work Performed Under Contract No. DE-AC21-86MC23075

For
U.S. Department of Energy
Office of Fossil Energy
Morgantown Energy Technology Center
Morgantown, West Virginia
Dr. Richard Johnson
COTR

By

Contractor

Advanced Fuel Research, Inc.
87 Church Street
East Hartford, CT 06108
(203) 528-9806

Program Director

Peter R. Solomon
President

Subcontractor

Brigham Young University
Provo, Utah 84602
(801) 378-4326

Program Director

L. Douglas Smoot
Dean and Professor

DISCLAIMER

PATENT STATUS

DOE/MC/23075--3151

DE93 004068

ABSTRACT

The overall objective of this program is the development of predictive capability for the design, scale up, simulation, control and feedstock evaluation in advanced coal conversion devices. This technology is important to reduce the technical and economic risks inherent in utilizing coal, a feedstock whose variable and often unexpected behavior presents a significant challenge. This program will merge significant advances made at Advanced Fuel Research, Inc. (AFR) in measuring and quantitatively describing the mechanisms in coal conversion behavior, with technology being developed at Brigham Young University (BYU) in comprehensive computer codes for mechanistic modeling of entrained-bed gasification. Additional capabilities in predicting pollutant formation will be implemented and the technology will be expanded to fixed-bed reactors.

The foundation to describe coal-specific conversion behavior is AFR's Functional Group (FG) and Devolatilization, Vaporization and Crosslinking (DVC) models, developed under previous and on-going METC sponsored programs. These models have demonstrated the capability to describe the time dependent evolution of individual gas species, and the amount and characteristics of tar and char. The combined FG-DVC model will be integrated with BYU's comprehensive two-dimensional reactor model, PCGC-2, which is currently the most widely used reactor simulation for combustion or gasification. The program includes: i) validation of the submodels by comparison with laboratory data obtained in this program, ii) extensive validation of the modified comprehensive code by comparison of predicted results with data from bench-scale and process scale investigations of gasification, mild gasification and combustion of coal or coal-derived products in heat engines, and iii) development of well documented user friendly software applicable to a "workstation" environment.

Success in this program will be a major step in improving the predictive capabilities for coal conversion processes including: demonstrated accuracy and reliability and a generalized "first principles" treatment of coals based on readily obtained composition data.

The progress during the twenty-third quarter of the program is summarized below.

For Subtask 2.a., The main objective of the work on char reactivity during the past quarter was to correlate the reactivity with pore structure measurements. It was found that high heating rates lead to chars of more porous structure in the case of bituminous coals. The lignite chars were found to have much higher surface areas and higher pore volumes than the bituminous chars. The work to date on the influence of char structure on reactivity was summarized in a paper prepared for presentation at the ACS Washington, D.C. Meeting.

Work continued on the sulfur and nitrogen experiments. A comparison was made for the NH_3 and HCN evolution from the Argonne coals between slow heating rate pyrolysis in the TG-FTIR and high heating rate pyrolysis in the Entrained Flow Reactor (EFR). For each coal, the total amount of nitrogen evolved in each of the pyrolysis systems is similar. The ratio of HCN to NH_3, however, differs significantly. The dominant product during slow heating rate pyrolysis in the TG-FTIR is NH_3 while the only observed product during rapid pyrolysis in the EFR is HCN. The work to date on the sulfur and nitrogen evolution experiments has been summarized in a paper prepared for presentation at the ACS Washington, D.C. Meeting. In addition, a modeling strategy was developed for the sulur and nitrogen evolution data.

For Subtask 2.b., The high-pressure, controlled-profile (HPCP) reactor, including the char, tar and gas separation and collection system, was extensively utilized in coal devolatilization, char preparation and char oxidation experiments. Approximately 90 oxidation tests of UT Blind Canyon HVB coal char were completed at 1, 5, 10 and 15 atm total pressure, with successful *in-situ* measurement of char particle size, velocity and temperature. Improved titanium analyses to determine char burnout were completed for most of the samples. Detailed analyses of the results are in progress and will be presented in the final report for this study.

For Subtask 2.c., Discussions continued with BYU on implementation of the soot oxidation and particle ignition submodels.

For Subtask 2.d., No work scheduled.

For Subtask 2.e., Work continued on exploring the reduced tar yields in high pressure gasifiers. In the previous quarterly, laboratory studies showed no evidence of tar gasification by CO_2 at temperatures between 800 and 1000 °C. However, significant tar cracking occured during post-pyrolysis in helium at similar temperatures, resulting in the formation of light hydrocarbon gases. In order to confirm this conclusion, the compositions of products from high pressure and atmospheric gasifiers were compared. The high pressure gasifier, which had a low tar yield, had a longer gas phase residence time, and increased yields of dust and CH_4. The average yields of tars, CH_4 and dust were compared. Interestingly enough, the total yields of tar, dust and CH_4 are close for the two different gasifiers. Consequently, it can be concluded that tar thermal cracking to form hydrocarbon light gases and dust (or soot) is primarily responsible for the low tar yields observed from the high pressure gasifiers.

For Subtask 2.f., Work continued on constructing the cantilever beam balance unit to be connected to an optical access port of the HPCP reactor. A theory was developed for correlating data from the large-particle tests at atmospheric pressure. Additional tests were performed. A paper was prepared and submitted for publication.

For Subtask 2.g., The submodel option for capturing H_2S was tested. Preparation of documentation for the user's manual was initiated.

For Subtask 3.a., A new equilibrium algorithm that allows for condensed phases was integrated into the 2-D code. A problem with the solid-gas momentum coupling was uncovered under independent work and corrected. Two cases of coal combustion in the BYU/ACERC controlled-profile reactor were re-simulated with reduced swirl numbers. Two cases of coal combustion in the Imperial College reactor were also simulated.

For Subtask 3.b., Work continued on developing and evaluating the fixed-bed model, FBED-1. The consolidation of data for the final simulations of a high pressure, Lurgi gasifier and an atmospheric pressure Wellman-Galusha gasifier was completed. The problem of extremely steep temperature gradients and devolatilization rates was resolved by properly modeling the energy exchange between the solid and the gas phases. An option to allow the thermal decomposition of tar in the gas phase was added. Major modifications in the code were made to improve the code structure and enhance user friendliness. Options were added in the fixed-bed code to choose among various devolatilization submodels, e.g., FG-DVC and FG-SET with a variable number of functional groups. Work on improving the zero-dimensional portion of the code was

initiated. A paper on fixed-bed modeling was published and a second was submitted.

For Subtask 3.c., Testing of this submodel was completed by simulating sidewall injection of sorbent with sulfur capture in a laboratory gasifier. The 2-D simulation over-predicted the degree of sulfur capture, presumably because of inadequately modeling the 3-D mixing effects of the sidewall injection.

For Subtask 4.a., One of the two application cases, namely, the Coal Tech cyclone combustor (a Clean Coal Technology project), was simulated with the updated version of the FG-DVC submodel.

For Subtask 4.b., Work continued on collecting fixed-bed design and test data from organizations and individuals involved in fixed- or moving-bed gasification or combustion research or in research on non-reacting fixed- or moving beds. No new data sets were obtained. Work also continued on collecting fixed-bed experimental data from the open literature.

"MEASUREMENT AND MODELING OF COAL CONVERSION PROCESSES"

Contract No. DE-AC21-86MC23075

Table of Contents

Reprints removed.

SECTION I. INTRODUCTION

I.A. PROGRAM BACKGROUND AND DESCRIPTION

During the past several years, significant advances have been made at Brigham Young University (BYU) in comprehensive two-dimensional computer codes for mechanistic modeling of entrained-bed gasification and pulverized coal combustion. During the same time period, significant advances have been made at Advanced Fuel Research, Inc. (AFR) in the mechanisms and kinetics of coal pyrolysis and secondary reactions of pyrolysis products. This program presents a unique opportunity to merge the technology developed by each organization to provide detailed predictive capability for advanced coal characterization techniques in conjunction with comprehensive computer models to provide accurate process simulations.

The program will streamline submodels existing or under development for coal pyrolysis chemistry, volatile secondary reactions, tar formation, soot formation, char reactivity, and SO_x-NO_x pollutant formation. Submodels for coal viscosity, agglomeration, tar/char secondary reactions, sulfur capture, and ash physics and chemistry will be developed or adapted. The submodels will first be incorporated into the BYU entrained-bed gasification code and subsequently, into a fixed-bed gasification code (to be selected and adapted). These codes will be validated by comparison with small scale laboratory and PDU-scale experiments. The validated code could then be employed to simulate and to develop advanced coal conversion reactors of interest to METC.

I.B. OBJECTIVES

The objectives of this study are to establish the mechanisms and rates of basic steps in coal conversion processes, to integrate and incorporate this information into comprehensive computer models for coal conversion processes, to evaluate these models and to apply them to gasification, mild gasification and combustion in heat engines.

I.C. APPROACH

This program is a closely integrated, cooperative effort between AFR and BYU. The program consists of four tasks: 1) Preparation of Research Plans, 2) Submodel

Development and Evaluation, 3) Comprehensive Model Development and Evaluation, and 4) Applications and Implementation.

I.D. CRITICAL TECHNICAL ISSUES

To achieve the goals of the program, the computer models must provide accurate and reliable descriptions of coal conversion processes. This will require the reduction of very complicated and interrelated physical and chemical phenomena to mathematical descriptions and, subsequently, to operational computer codes. To accomplish this objective, a number of technical issues must be addressed as noted below. The status of each of these tasks is also included:

A Separation of Rates for Chemical Reaction, Heat Transfer, and Mass Transfer
A Particle Temperature Measurements Using FT-IR E/T Spectroscopy
A Functional Group Description of Coal, Char and Tar
A Tar Formation Mechanisms
A Char Formation Mechanisms
A Viscosity/Swelling
A Intraparticle Transport
A Pyrolysis of Volatiles and Soot Formation
A Secondary Reaction of Tar
A Particle Ignition
A Char Reactivity
I Ash Chemistry and Physics
A Particle Optical Properties
A Coupling of Submodels with Comprehensive Codes
I Comprehensive Code Efficiency
I Turbulence
A SO_x and NO_x
A Generalized Fuels Models
A Fixed-Bed Model

(o) to be addressed; (I) initiated; (A) almost completed; (C) completed. These technical issues are addressed in the three Tasks as described in Sections II-IV.

I.E. TWENTY-THIRD QUARTER PROGRESS

Subtask 2.a. Coal to Char Chemistry Submodel Development and Evaluation

The main objective of the work on char reactivity during the past quarter was to correlate the reactivity with pore structure measurements. In an attempt to characterize the pore structure of the chars studied, nitrogen adsorption measurements were performed using a Quantasorb instrument. The data at 0% burnoff provide useful information on the number and accessibility of the mesopores of the char. The adsorption data at higher burnoffs provide an indication of the amount of microporosity present.

It was found that high heating rates lead to chars of more porous structure in the case of bituminous coals. The lignite chars were found to have much higher surface areas and higher pore volumes than the bituminous chars. The work to date on the influence of char structure on reactivity was summarized in a paper prepared for presentation at the ACS Washington, D.C. Meeting (August 23-28, 1992). It is included as Appendix A of this report.

Work continued on the sulfur and nitrogen experiments. Additional TG-FTIR runs with post-oxidation of volatile products were done with pure pyrite in the presence of various gases to see if any of these cause a reduction in the pyrite decomposition temperature or a splitting into two peaks. So far, CO_2, CO, H_2O, and H_2 have been tested with no apparent effect. Since for each Argonne Premium coal the tar evolution and the low temperature SO_2 evolution have similar T_{max}'s, it is possible that the tars are responsible for the low temperature pyrite decomposition in coal. Arrhenius plots show that the mean tar and low temperature SO_2 reaction rates differ by a factor of 4 for the Illinois #6 coal and are virtually identical for the Pittsburgh #8 coal.

A comparison was made for the NH_3 and HCN evolution from the Argonne coals between slow heating rate pyrolysis in the TG-FTIR and high heating rate pyrolysis in the Entrained Flow Reactor (EFR). For each coal, the total amount of nitrogen evolved in each of the pyrolysis systems is similar. The ratio of HCN to NH_3, however, differs significantly. The dominant product during slow heating rate pyrolysis in the TG-FTIR is NH_3 while the only observed product during rapid pyrolysis in the EFR is HCN.

The work to date on the sulfur and nitrogen evolution experiments has been summarized in a paper prepared for presentation at the ACS Washington, D.C. Meeting (August 23-28, 1992). It is included as Appendix B of this report. In addition, a modeling strategy was developed for the sulur and nitrogen evolution data.

Work also continued on the swelling model. Work continues in two directions: 1) the dependence of the swelling amount on ambient pressure, for high fluidity coals; 2) extrapolating the swelling behavior of large particles (>100 μm) using the current single bubble model. A drop tube experiment was planned to obtain data on the effect of particle size on swelling, so the current single bubble model (small particles) can be extended to the multi-bubble case (large particles).

Subtask 2.b. Fundamental High-Pressure Reaction Rate Data

The high-pressure, controlled-profile (HPCP) reactor, including the char, tar and gas separation and collection system, was extensively utilized in coal devolatilization, char preparation and char oxidation experiments. Approximately 90 oxidation tests of UT Blind Canyon HVB coal char were completed at 1, 5, 10 and 15 atm total pressure, with successful *in-situ* measurement of char particle size, velocity and temperature. Improved titanium analyses to determine char burnout were completed for most of the samples. Detailed analyses of the results are in progress and will be presented in the final report for this study.

Subtask 2.c. Secondary Reaction of Pyrolysis Products and Char Burnout

Discussions continued with BYU on implementation of the soot oxidation and particle ignition submodels.

Subtask 2.d. Ash Physics and Chemistry Submodel

No work scheduled.

Subtask 2.e. Large Particle Submodels

Work continued on exploring the reduced tar yields in high pressure gasifiers.

In the previous quarterly, laboratory studies showed no evidence of tar gasification by CO_2 at temperatures between 800 and 1000 °C. However, significant tar cracking occured during post-pyrolysis in helium at similar temperatures, resulting in the formation of light hydrocarbon gases (CH_4, C_2H_4, C_2H_2, ..., etc.). In order to confirm this conclusion, the compositions of products from high pressure and atmospheric gasifiers were compared.

For a fair comparison, mass balance calculations using data in an EPRI report (GS-6797, Oct., 1990) were done on a high pressure (300 psig, GE) and an atmospheric (MIFGa/USBM) gasifiers, both of which used Illinois coal as feedstock and were operated at similar coal and air input rates for several runs, although the high pressure gasifier had a higher steam input. The high pressure gasifier, which had a low tar yield, had a longer gas phase residence time, and increased yields of dust and CH_4. The average yields of tars, CH_4 and dust were compared. Interestingly enough, the total yields of tar, dust and CH_4 are close for the two different gasifiers. Consequently, it can be concluded that tar thermal cracking to form hydrocarbon light gases and dust (or soot) is primarily responsible for the low tar yields observed from the high pressure gasifiers.

Subtask 2.f. Large Char Particle Oxidation at High Pressure

Work continued on constructing the cantilever beam balance unit to be connected to an optical access port of the HPCP reactor. A theory was developed for correlating data from the large-particle tests at atmospheric pressure. Additional tests were performed. A paper was prepared and submitted for publication.

Subtask 2.g. SO_x - NO_x Submodel Development

The submodel option for capturing H_2S was tested. Preparation of documentation for the user's manual was initiated.

Subtask 3.a. Integration of Advanced Submodels into Entrained-Flow Code, with Evaluation and Documentation

A new equilibrium algorithm that allows for condensed phases was integrated into

the 2-D code. A problem with the solid-gas momentum coupling was uncovered under independent work and corrected. Two cases of coal combustion in the BYU/ACERC controlled-profile reactor were re-simulated with reduced swirl numbers. Two cases of coal combustion in the Imperial College reactor were also simulated.

Subtask 3.b. Comprehensive Fixed-Bed Modeling Review, Development, Evaluation, and Implementation

Work continued on developing and evaluating the fixed-bed model, FBED-1. The consolidation of data for the final simulations of a high pressure, Lurgi gasifier and an atmospheric pressure Wellman-Galusha gasifier was completed. The problem of extremely steep temperature gradients and devolatilization rates was resolved by properly modeling the energy exchange between the solid and the gas phases. An option to allow the thermal decomposition of tar in the gas phase was added. Major modifications in the code were made to improve the code structure and enhance user friendliness. Options were added in the fixed-bed code to choose among various devolatilization submodels, e.g., FG-DVC and FG-SET with a variable number of functional groups. Work on improving the zero-dimensional portion of the code was initiated. A paper on fixed-bed modeling was published and a second was submitted.

Subtask 3.c. Generalized Fuels Feedstock Submodel

Testing of this submodel was completed by simulating sidewall injection of sorbent with sulfur capture in a laboratory gasifier. The 2-D simulation over-predicted the degree of sulfur capture, presumably because of inadequately modeling the 3-D mixing effects of the sidewall injection.

Subtask 4.a. Application of Generalized Pulverized Coal Comprehensive Code

One of the two application cases, namely, the Coal Tech cyclone combustor (a Clean Coal Technology project), was simulated with the updated version of the FG-DVC submodel.

Subtask 4.b. Application of Fixed-Bed Code

Work continued on collecting fixed-bed design and test data from organizations and individuals involved in fixed- or moving-bed gasification or combustion research or in research on non-reacting fixed- or moving beds. No new data sets were obtained. Work also continued on collecting fixed-bed experimental data from the open literature.

SECTION II. TASK 2. SUBMODEL DEVELOPMENT AND EVALUATION

Objectives

The objectives of this task are to develop or adapt advanced physics and chemistry submodels for the reactions of coal in an entrained-bed and a fixed-bed reactor and to validate the submodels by comparison with laboratory scale experiments.

Task Outline

The development of advanced submodels for the entrained-bed and fixed-bed reactor models will be organized into the following categories: a) Coal Chemistry (including coal pyrolysis chemistry, char formation, particle mass transfer, particle thermal properties, and particle physical behavior); b) Char Reaction Chemistry at high pressure; c) Secondary Reactions of Pyrolysis Products (including gas-phase cracking, soot formation, ignition, char burnout, sulfur capture, and tar/gas reactions); d) Ash Physics and Chemistry (including mineral characterization, evolution of volatile, molten and dry particle components, and ash fusion behavior); e) Large Coal Particle Effects (including secondary reactions within the particle and in multiple particle layers; f) Large Char Particle Effects (including oxidation); g) SO_x-NO_x Submodel Development (including the evolution and oxidation of sulfur and nitrogen species); and h) SO_x and NO_x Model Evaluation.

II.A. SUBTASK 2.a. - COAL TO CHAR CHEMISTRY SUBMODEL DEVELOPMENT AND EVALUATION

Senior Investigators - David G. Hamblen and Michael A. Serio
-Advanced Fuel Research, Inc.
87 Church Street, East Hartford, CT 06108
(203) 528-9806

Objective

The objective of this subtask is to develop and evaluate, by comparison with laboratory experiments, an integrated and compatible submodel to describe the organic chemistry and physical changes occurring during the transformation from coal to char in coal conversion processes.

Accomplishments

The main objective of the work on char reactivity during the past quarter was to correlate the reactivity with pore structure measurements. In an attempt to characterize the pore structure of the chars studied, nitrogen adsorption measurements were performed using a Quantasorb instrument. The data at 0% burnoff provide useful information on the number and accessibility of the mesopores of the char. The adsorption data at higher burnoffs provide an indication of the amount of microporosity present.

The chars studied included: a low heating rate Pittsburgh No.8 (Pitts8 TGA), a high heating rate Pittsburgh No.8 (Pitts8 EFR), a low heating rate Zap lignite (Zap TGA) and a low heating rate demineralized Zap lignite (Zapd TGA). The results show that the Pitts8 EFR char has a higher surface area (at both 0% and higher burnoff) and cumulative pore volume (measured at 0% burnoff, corresponding to the mesopores volume) than the Pitts8 TGA, which implies that it has a more "open" structure. This observation is consistent with the fact that the Pitts8 TGA char reaches the pore diffusion regime before the Pitts8 EFR char. Since the two chars were produced at different heating rates, it can be concluded that high heating rates lead to chars of more porous structure. The Zap TGA and Zapd TGA chars were found to have much higher surface areas and higher pore volumes than the Pitts8 chars. The work to date on the

influence of char structure on reactivity was summarized in a paper prepared for presentation at the ACS Washington, D.C. Meeting (August 23-28, 1992). It is included as Appendix A of this report.

Work continued on the sulfur and nitrogen experiments. Additional TG-FTIR runs with post-oxidation of volatile products were done with pure pyrite in the presence of various gases to see if any of these cause a reduction in the pyrite decomposition temperature or a splitting into two peaks. So far, CO_2, CO, H_2O, and H_2 have been tested with no apparent effect. Since for each Argonne Premium coal the tar evolution and the low temperature SO_2 evolution have similar T_{max}'s, it is possible that the tars are responsible for the low temperature pyrite decomposition in coal. Arrhenius plots show that the mean tar and low temperature SO_2 reaction rates differ by a factor of 4 for the Illinois #6 coal and are virtually identical for the Pittsburgh #8 coal.

The TG-FTIR was recalibrated for HCN using an 11 ppm HCN in Helium gas cylinder. The Nicolet spectrometer was also calibrated for HCN using the same HCN gas cylinder to allow comparison between the slow heating rate pyrolysis in the TG-FTIR to the high heating rate pyrolysis data in the Entrained Flow Reactor (EFR). For each coal, the total amount of nitrogen evolved in each of the pyrolysis systems is similar. The ratio of HCN to NH_3, however, differs significantly. The dominant product during slow heating rate pyrolysis in the TG-FTIR is NH_3 while the only observed product during rapid pyrolysis in the EFR is HCN.

The work to date on the sulfur and nitrogen evolution experiments has been summarized in a paper prepared for presentation at the ACS Washington, D.C. Meeting (August 23-28, 1992). It is included as Appendix B of this report.

A modeling strategy was developed for the sulur and nitrogen evolution data which can be summarized as follows:

1) Organic sulfur decomposes into three gases, H_2S, COS, and SO_2. H_2S is the major species, and contributes to both the first and second peaks(to be tested). COS has its contribution under the first peak and SO_2 under the second peak, but they are minor species and will be treated as being in the background of the H_2S evolution. Therefore, H_2S will be the only individual species to be modeled, and

the predicted COS and SO_2 amounts may not represent their real yields but a lump sum of all background sulfur evolutions other than H_2S.

2) Pyrite decomposes to FeS, H_2S, COS and SO_2 under the second peak. H and C are donated by the aliphatic portion of coals and O is taken from oxygen groups. Alternative reactions of pyrite at either lower or higher temperatures are not considered. FeS decomposition is slow in pyrolysis and it will be assumed to be stable under these conditions.

3) The rank dependence of the sulfur evolution is to be modeled in two ways. Firstly, rank dependent evolution kinetics(activation energies) will be used for all the sulfur gases and for the pyrite decomposition to represent the shift of evolution temperatures toward higher temperatures with rank. Secondly, the amount of H_2S from organic sulfur under the two peaks will be adjusted to model the decay of the first peak at high coal ranks.

4) For very high rank coals like Pocahontas #3, strong bonding prevents a large extent of the organic sulfur evolution, and therefore, a larger portion of sulfur will be retained in the chars.

Work also continued on the swelling model. Work continues in two directions: 1) the dependence of the swelling amount on ambient pressure, for high fluidity coals; 2) extrapolating the swelling behavior of large particles (>100 μm) using the current single bubble model. A drop tube experiment was planned to obtain data on the effect of particle size on swelling, so the current single bubble model (small particles) can be extended to the multi-bubble case (large particles).

Char Reactivity

The main objective of the work during the past quarter was to correlate the char reactivity with pore structure measurements. In an attempt to characterize the pore structure of the chars studied, nitrogen adsorption measurements were performed using a Quantasorb instrument. From the adsorption isotherms, the N_2 surface areas (using the BET equation) and the cumulative pore volumes (using the Kelvin equation) were calculated. The data at 0% burnoff provide useful information on the number and

accessibility of the mesopores of the char. Since mesopores probably constitute the main pathway for oxygen to penetrate into the particle, their characterization is an important step in order to predict diffusion limitations. The adsorption data at higher burnoffs provide an indication of the amount of microporosity present.

The chars studied included: a low heating rate Pittsburgh No.8 (Pitts8 TGA), a high heating rate Pittsburgh No.8 (Pitts8 EFR), a low heating rate Zap lignite (Zap TGA) and a low heating rate demineralized Zap lignite (Zapd TGA). Table II.A-1 summarizes the char formation conditions and the corresponding surface areas, obtained at 0% burnoff and 10 or 35% burnoff. The cumulative pore volumes (at 0% burnoff) for the Pitts8 chars and the Zap TGA chars are shown in Fig II.A-1. The results show that the Pitts8 EFR char has a higher surface area (at both 0% and higher burnoff) and cumulative pore volume (measured at 0% burnoff, corresponding to the mesopores volume) than the Pitts8 TGA, which implies that it has a more "open" structure. This observation is consistent with the fact that the Pitts8 TGA char reaches the pore diffusion regime before the Pitts8 EFR char. Since the two chars were produced at different heating rates, it can be concluded that high heating rates lead to chars of more porous structure. Similarly, Su and Perlmutter (1985) arrived at the conclusion that chars with different pore structure can be generated from the same coals by varying pyrolysis conditions: a higher pyrolysis temperature or a slower heating rate generates chars of more compact structure. As indicated in Table II.A-1 and Fig II.A-1 the Zap TGA and Zapd TGA chars were found to have much higher surface areas and higher pore volumes than the Pitts8 chars. This is consistent with the results from Tseng and Edgar (1984,1985) who found that, for the same particle size, a bituminous char entered the diffusion limited regime before a lignite char. A more quantitative correlation of the pore volume with the degree of diffusion limitations will require additional data in the pore diffusion regime for the highly porous chars. Adsorption isotherms of chars with a certain degree of burnoff (10% for Pitts8 TGA and 35% for Pitts8 EFR) were obtained, and were found to be characteristic of a microporous structure, with most of the pores being smaller than 20 Å. In that case, the Kelvin equation cannot be utilized to calculate the pore volume, but the N_2 surface area obtained from the BET equation is thought to be representative of the amount of micropores present.

TABLE II.A-1 Char Properties

Char	Coal	Reactor	Heating Rate (°C/s)	Final Temp.(°C)	Char Particle Size (μm)	N_2 Surface Area (m^2/g)
Pitts8 TGA	Pitts 8	TGA	0.5	900	800 ± 200* 150 ± 50	0% BO:0.5 10% BO:98
Pitts8 EFR	Pitts 8	EFR	5000	1100	130 ± 30	0% BO:4 35% BO:310
Zap TGA	Zap	TGA	0.5	900	80 ± 40	0% BO:84
Zapd TGA	Zap	TGA	0.5	900	60 ± 20	0% BO:100

* In that case, the combustion cycle was performed immediately after the pyrolysis. The particle size is approximate, since the chars showed a cenospheric agglomerated structure.

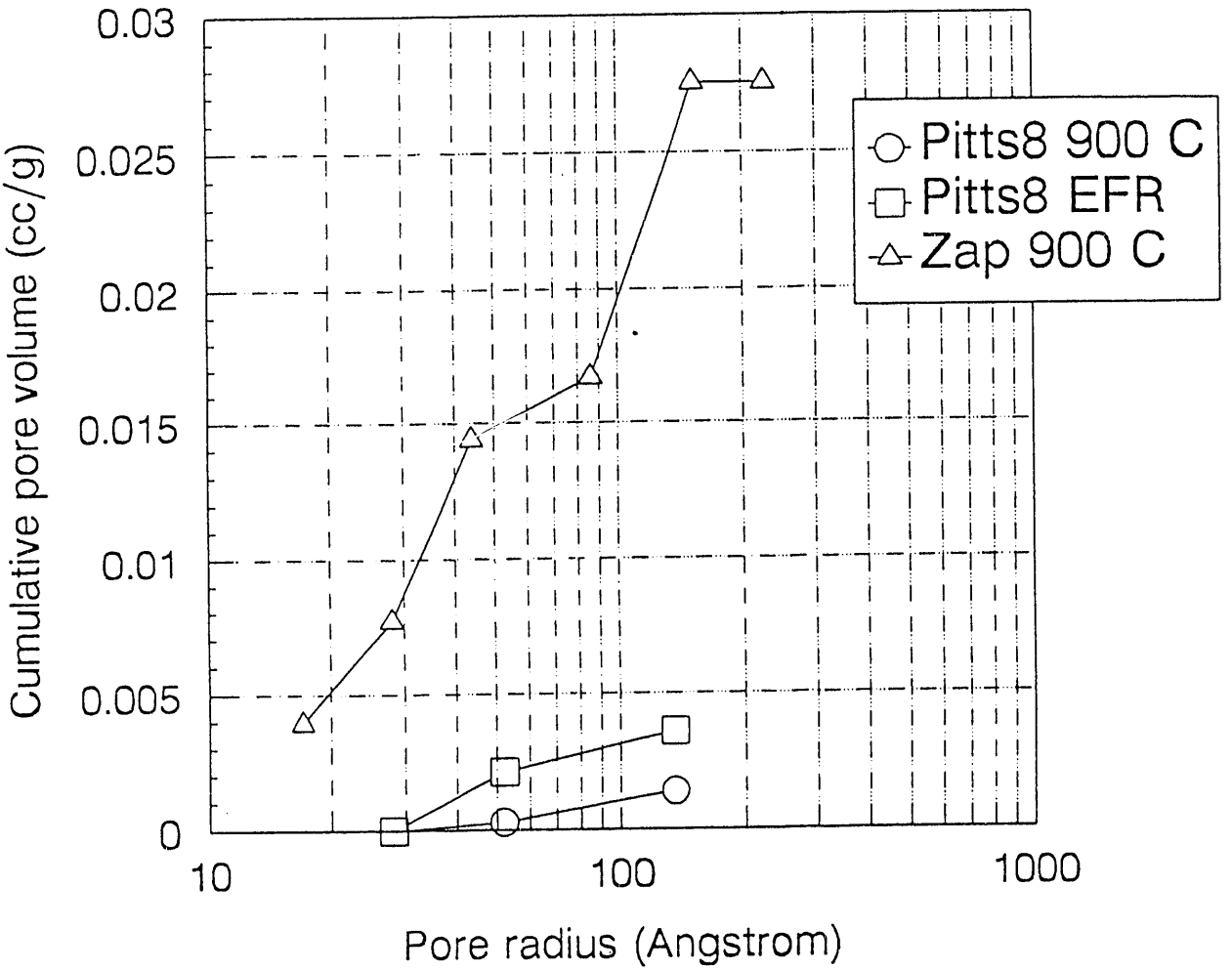

Figure II.A-1. Cumulative Pore Volume for PITTS8 EFR, PITTS8 TGA and ZAP TGA Chars.

The work to date was summarized in a paper prepared for presentation at the ACS Washington, D.C. Meeting (August 23-28, 1992). It is included as Appendix A of this report.

Sulfur and Nitrogen Evolution

Experimental Work

Work continued on the sulfur and nitrogen experiments. Additional TG-FTIR runs with post-oxidation of volatile products were done with pure pyrite in the presence of various gases to see if any of these cause a reduction in the pyrite decomposition temperature or a splitting into two peaks. So far, CO_2, CO, H_2O, and H_2 have been tested with no apparent effect. We expect that the pyrite may interact with hydrogen atoms which are donated from the coal structure. Ethane was therefore tested, however, ethane decomposition, which is known to produce hydrogen radicals, did not occur until after pyrite decomposition. Polymers which decompose in a similar temperature range as coal and produce hydrogen radicals will be tested next.

What causes the low temperature pyrite decomposition in coals during pyrolysis? Since for each Argonne Premium coal the tar evolution and the low temperature SO_2 evolution have similar T_{max}'s, it is possible that the tars are responsible for the low temperature pyrite decomposition in coal. In support of this possibility, presented in Fig. II.A-2 are Arrhenius plots comparing the mean reaction rates (r) for tar evolution and low temperature SO_2 evolution for Illinois #6 and Pittsburgh #8 coals respectively. The Arrhenius parameters were generated using the method of evaluating the T_{max} shift with heating rate. In this method, a plot of $\ln H_r/T_{max}^2$ versus $1/T_{max}$, where H_r is the experimental heating rate, produces a line with the slope equal to $-(E_a/R)$. The Arrhenius plots show that the mean tar and low temperature SO_2 reaction rates differ by a factor of 4 for the Illinois #6 coal and are virtually identical for the Pittsburgh #8 coal.

The TG-FTIR was recalibrated for HCN using an 11 ppm HCN in Helium gas cylinder. The Nicolet spectrometer was also calibrated for HCN using the same HCN gas cylinder to allow comparison between the slow heating rate pyrolysis in the TG-FTIR to the high heating rate pyrolysis data in the Entrained Flow Reactor (EFR).

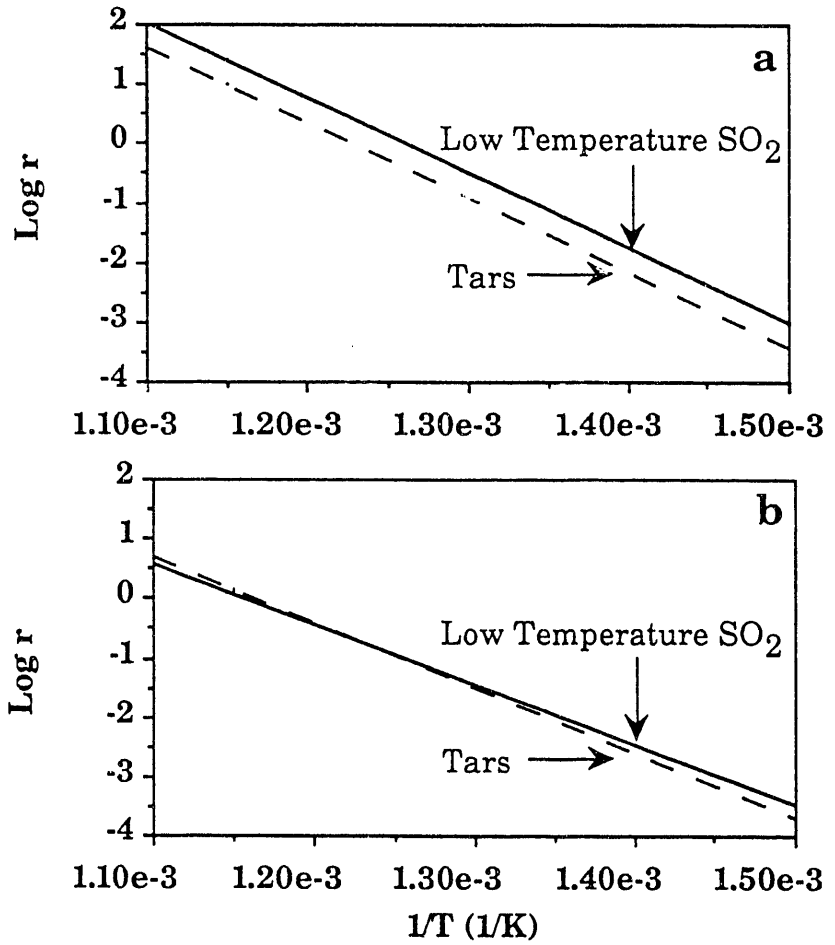

Figure II.A-2. Arrhenius Plots Comparing Mean Reaction Rate (r) of Tar Evolution and Low Temperature SO_2 Evolution for a) Illinois No. 6 and b) Pittsburgh No. 8.

The NH_3 and HCN weight percents are presented in Table II.A-2. For each coal, the total amount of nitrogen evolved in of the each pyrolysis systems is similar. The ratio of HCN to NH_3, however, differs significantly. The dominant product during slow heating rate pyrolysis in the TG-FTIR is NH_3 while the only observed product during rapid pyrolysis in the EFR is HCN. These results can be explained by the following possibilities: 1) A competitive reaction process leads to the formation of NH_3 at the expense of HCN at low pyrolysis heating rates; 2) In the entrained flow reactor, secondary pyrolysis reactions especially tar cracking, lead to the formation of HCN and the destruction of NH_3; 3) NH_3 is removed in the collection system in the entrained flow reactor (e.g., dissolution into water which condenses on the walls of the gas collection bag).

The work to date on the sulfur and nitrogen evolution experiments has been summarized in a paper prepared for presentation at the ACS Washington, D.C. Meeting (August 23-28, 1992). It is included as Appendix B of this report.

Table II.A-2
Summary of Data on HCN and NH_3 Evolution from Low Heating Rate (TG-FT-IR) and High Heating Rate (EFR) Experiments

	TG-FTIR (as received wt. %)		EFR 1100°C, 24" (ash free wt. %)	
	HCN	NH_3	HCN	NH_3
Pocahontas	0.034	0.27	0.28	0
Upper Freeport	0.028	0.42	0.78	0
Pittsburgh	0.038	0.47	0.84	0
Stockton	0.051	0.45	0.55	0
Utah Blind Canyon	0.101	0.53	1.21	0
Illinois	0.065	0.45	- - -	- - -
Wyodak	0.035	0.28	0.60	0
Zap	0.082	0.40	- - -	- - -

Modeling

Coal Sulfur Decompositions During Pyrolysis - The phenomenon of coal sulfur decomposition is complicated by the various forms of sulfur existing in the coal structure on one hand and the various gas species produced by the decomposition on the other. The absence of H_2S, which is believed to be a major product, from FT-IR spectra makes the understanding of the physical and chemical nature of this process more difficult. Nevertheless, some progress has been made in analyzing the data of the runs from the TG-FTIR system using the post-oxidizer attachment (in which sulfur species are converted to SO_2 which is easily detected), along with the COS and SO_2 evolutions from standard pyrolysis runs in the TG-FTIR. A preliminary understanding of this phenomenon has been reached and modeling has begun. The following discussions are based on the results of pyrolysis and post oxidized runs at 30°C/min for the eight Argonne coals and four PSOC Hvb coals which have low pyrite contents.

Sulfur exists in coals in three forms: organic sulfur, pyritic sulfur, and sulfates. Organic sulfur is in the coal structure, either in aromatic rings or in the aliphatic portion. Pyrite exists in coal as dispersed particles, but interactions with the coal structure to a certain extent are expected. Sulfates are believed to be only a very small part of the total sulfur in most of coals, especially for coals from the Argonne Premium Coal Sample Bank (Vorres, 1990), and therefore, can be ignored in the current project.

Organic vs Pyritic Sulfur - During devolatilization, sulfur in various forms decomposes into gas species, including H_2S, COS, SO_2 and CS_2, and a large amount of it will remain in the char and then be evolved in the combustion cycle. Some of the sulfur will be evolved with the tar as other gas pools, and it does not constitute a modeling problem here. Pyrite FeS_2 is believed to decompose mainly as $FeS_2 \rightarrow FeS + S$, and further reaction of FeS is slow during pyrolysis. Alternative pyrite reactions with coal gases are possible as suggested by Khan (1989), but they may be less significant. S from FeS_2 decomposition will react with the coal structure, forming all the possible sulfur gas species listed above.

As discussed above and in the 22nd quarterly report, the SO_2 evolution in a post oxidized run has two peaks during pyrolysis. The second peak is sharp and coincides with the pure pyrite decomposition temperature, so it is believed to be mainly due to pyrite devolatilization. The amount of sulfur that evolves under these two peaks for the eight Argonne coals is listed in Table II.A-3. The experimental conditions were described in the previous quarterly report. In Figure II.A-3, the ratio of the sulfur amount under the second peak to the pyritic sulfur in the coal is plotted for the eight Argonne coals. With the exception of the Zap and Pocahontas #3, this ratio is consistently around 0.5 and is not affected significantly by the variation of the total organic sulfur content. This implies that the contribution of organic sulfur to the second peak is insignificant and that the major contributor to the first peak is the organic sulfur, which is primarily evolved as H_2S. SO_2 from organic sulfur may evolve at higher temperatures and be part of the second peak (see discussion below).

The fraction of the sulfur amount under the first peak, when compared to the organic sulfur content, steadily decreases as coal rank increases, as seen in Fig. II.A-4, indicating a possible increase in the bonding of organic sulfur to the coal structure during the coalification. But as plotted in Fig. II.A-5, the ratio of the total sulfur evolved in post oxidized pyrolysis to the total sulfur contents of the eight Argonne coals maintains a constant value of about 0.5, except for Pocahontas #3 and Zap. It may mean that, for most of coals, the contributions from organic sulfur to the first peak could decrease as coal rank increases, while those to the second peak increase.

Decomposition Product Distribution - The CS_2 evolution amount during a standard pyrolysis run is as low as 0.02wt% and therefore is ignored in the current model.

The percentages of SO_2 and COS are higher than for CS_2 but still very low, and they are basically a background evolution under the H_2S peaks. Their evolutions during pyrolysis exhibit a very random nature with multiple peaks as illustrated in Fig. II.A-6. Some peaks are at temperatures as high as 800°C, which is much higher than the temperature range of 400°C to 600°C, normally assumed for sulfur decomposition. This model will not consider such high temperature behavior but will be based on the two-peak framework presented above.

Table II.A-3 The Amounts of Sulfur Evolved under the Two Peaks during Pyrolysis, wt% of DAF Coals.

Coals	1st Peak	2nd Peak
Zap	0.329	0.199
Wyodak	0.339	0.096
Illinois #6	1.429	1.594
Utah	0.184	0.128
Stockton	0.2537	0.132
Pittsburgh Seam	0.404	0.902
Upper freeport	0.190	1.340
Pocahontas #3	0.075	0.046

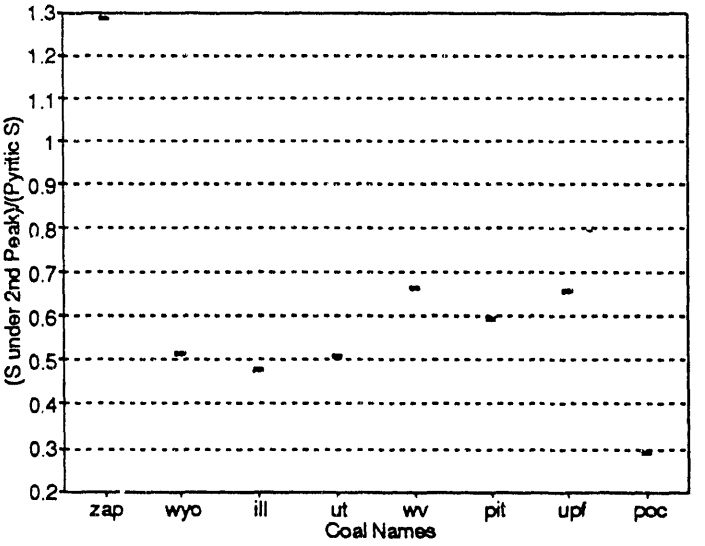

Figure II.A-3. The Ratios of Sulfur Evolved Under the Second Peak to Pyrite Sulfur Contents of Eight Argonne Coals.

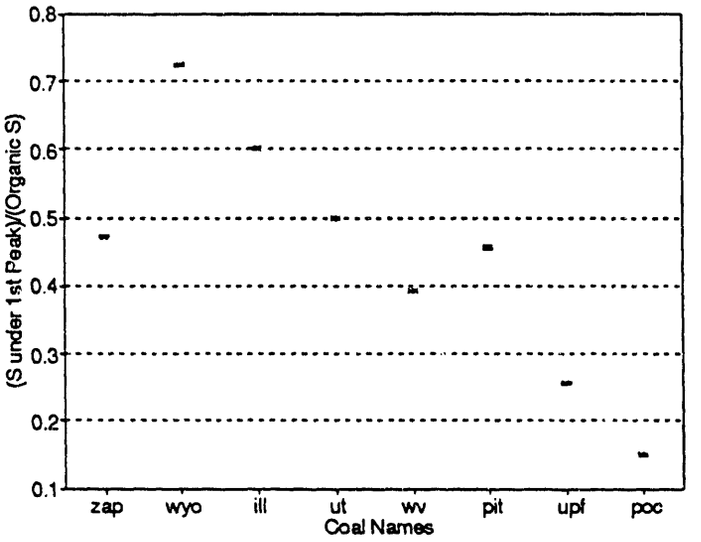

Figure II.A-4. The Ratios of Sulfur Evolved Under the First Peak to Organic Sulfur Contents of Eight Argonne Coals.

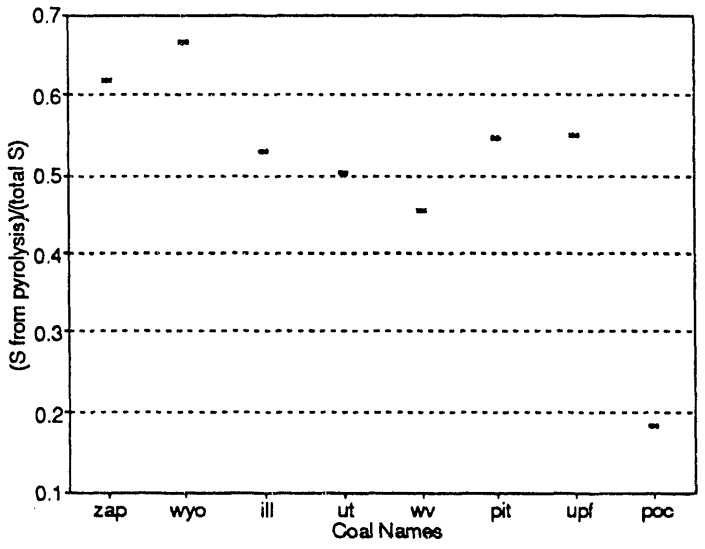

Figure II.A-5. The Ratios of Sulfur Evolved in the Post-Oxidized Pyrolysis to the Total Sulfur Contents of Eight Argonne Coals.

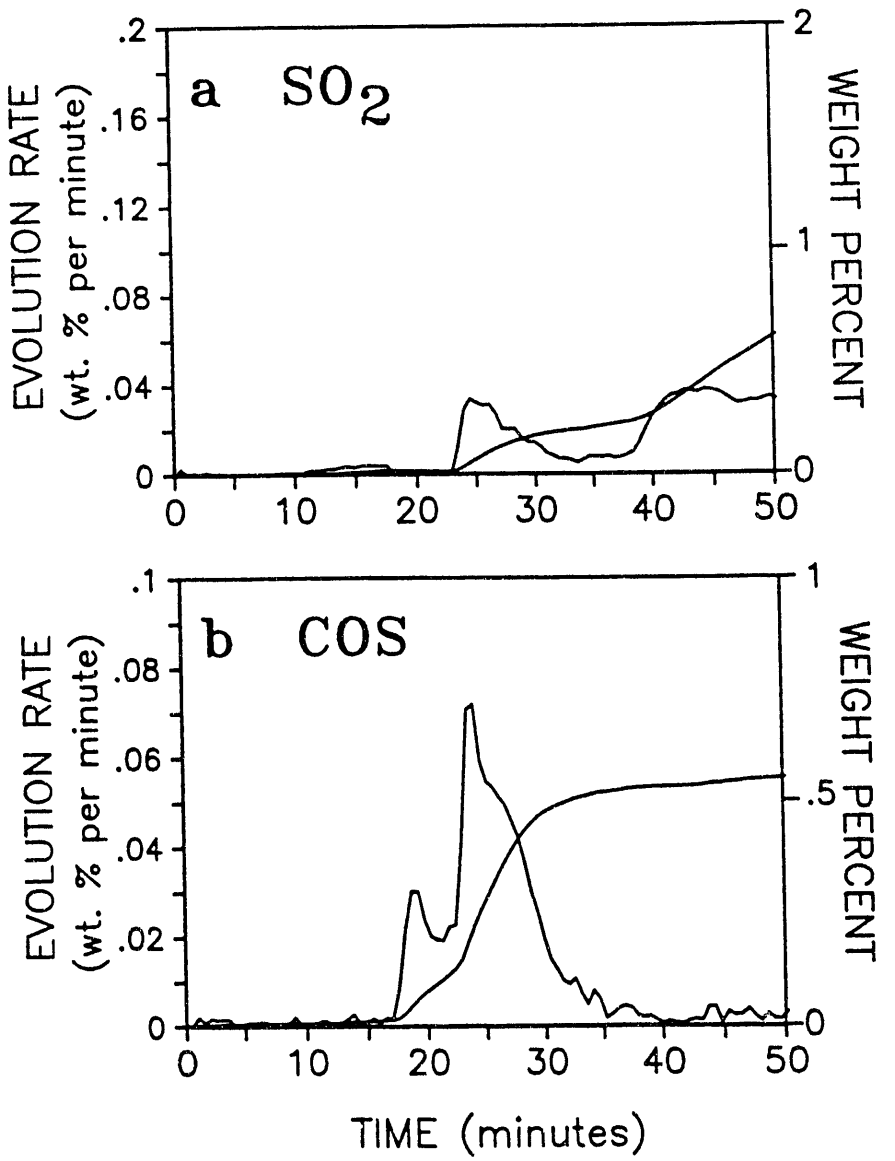

Figure II.A-6. Evolutions of a) SO_2 and b) COS of an Illinois No. 6 Coal at a Heating Rate of 30°C/min.

Analysis of the normal SO_2 pyrolysis evolutions from the eight Argonne coals reveals that, with one exception, SO_2 starts to evolve at temperatures around 580°C. Its amount constitutes about 5% of the total sulfur in the coals and it appears to derive from both mineral and organic sources (see Fig. II.A-7). The SO_2 amounts from the four PSOC coals are almost zero except for PSOC 1522 which has 0.52wt% pyrite sulfur. Consequently, for high rank coals, SO_2 may come from pyrite sulfur only.

COS evolution curves have two major peaks at about 400°C and 560°C, which could correspond to organic and pyritic sulfur respectively. Khan (1989) has concluded in his study of a group of bituminous coals that sulfur evolved as COS in pyrolysis has 4% of the pyritic and 6.3% of the organic sulfur. However, the amount of COS evolved as a fraction of the total sulfur evolution decreases with coal rank as plotted in Fig. II.A-8. An examination of the COS evolution curves for the eight Argonne coals reveals that the low temperature COS peak decays at high coal ranks and moves toward higher temperatures. It will be assumed that COS will contain 0% to 10% of organic sulfur depending on the coal rank and 4% of the pyritic sulfur.

H_2S is the major sulfur gas species, but it cannot be detected with FTIR. Coburn et al. (1991) and Kelemen et al. (1991) have shown that the H_2S evolution has the same appearance as the post oxidized run results, i.e., a broad first peak and a sharp second peak. The H_2S evolutions for the eight Argonne coals determined by Kelemen et al. (1991) show a reduction of the first H_2S peak with rank which is consistent with the first peak of the SO_2 evolution in post oxidized runs. We can now correlate the first peak to the organic sulfur and the second to the pyrite, but there may also be a small amount of H_2S from the organic sulfur under the second peak, i.e., H_2S from the organic sulfur may have a loose pool and a tight pool. The loose pool is the major pool but its amount decreases with rank. This postulation will be tested for coals with low pyrite content like PSOC 1474.

<u>Modeling Strategies</u> - Based on the above discussions, the current modeling strategies are:

1) Organic sulfur decomposes into three gases, H_2S, COS, and SO_2. H_2S is the major species, and contributes to both the first and second peaks(to be tested). COS has its contribution under the first peak and SO_2 under the second peak, but they are minor species and will be treated as being in the background of the H_2S

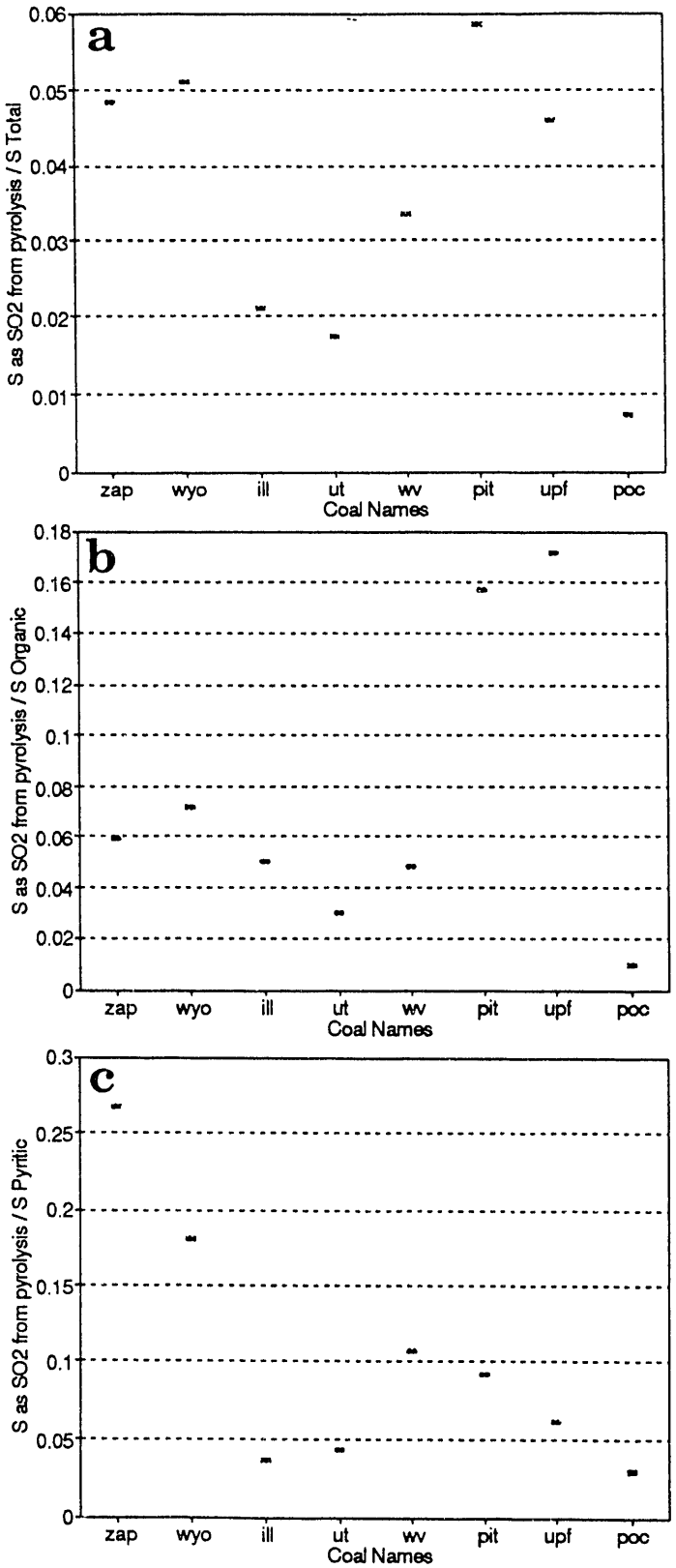

Figure II.A-7. The Ratios of Sulfur Evolved as SO_2 to a) Total Sulfur Contents, b) Organic Sulfur Contents, and c) Pyritic Sulfur Contents of Eight Argonne Coals.

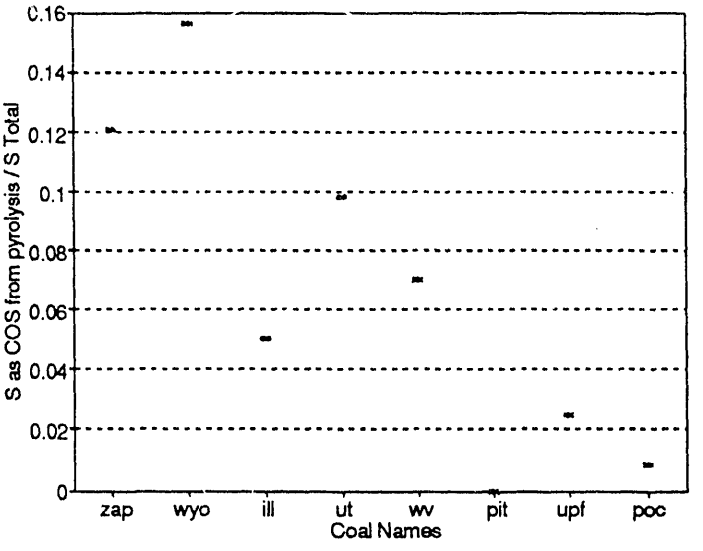

Figure II.A-8. The Ratios of Sulfur Evolved as COS to Total Sulfur Contents of Eight Argonne Coals.

evolution. Therefore, H_2S will be the only individual species to be modeled, and the predicted COS and SO_2 amounts may not represent their real yields but a lump sum of all background sulfur evolutions other than H_2S.

2) Pyrite decomposes to FeS, H_2S, COS and SO_2 under the second peak. H and C are donated by the aliphatic portion of coals and O is taken from oxygen groups. Alternative reactions of pyrite at either lower or higher temperatures are not considered. FeS decomposition is slow in pyrolysis and it will be assumed to be stable under these conditions.

3) The rank dependence of the sulfur evolution is to be modeled in two ways. Firstly, rank dependent evolution kinetics(activation energies) will be used for all the sulfur gases and for the pyrite decomposition to represent the shift of evolution temperatures toward higher temperatures with rank. Secondly, the amount of H_2S from organic sulfur under the two peaks will be adjusted to model the decay of the first peak at high coal ranks.

4) For very high rank coals like Pocahontas #3, strong bonding prevents a large extent of the organic sulfur evolution, and therefore, a larger portion of sulfur will be retained in the chars.

The major unknown at this stage is whether there is a heating rate dependence of sulfur evolution, and if there is, how to model it.

Swelling Model

Work also continued on the swelling model. Work continues in two directions: 1) the dependence of the swelling amount on ambient pressure, for high fluidity coals; 2) extrapolating the swelling behavior of large particles (>100 μm) using the current single bubble model. A drop tube experiment was planned to obtain data on the effect of particle size on swelling, so the current single bubble model (small particles) can be extended to the multi-bubble case (large particles).

Plans

Complete work on the sub-models for swelling, char reactivity and the evolution of sulfur and nitrogen species. Complete documentation for User's Manual.

II.B. SUBTASK 2.B. - FUNDAMENTAL HIGH-PRESSURE REACTION RATE DATA

Senior Investigators - Geoffrey J. Germane and Angus U. Blackham
Brigham Young University
Provo, Utah 84602
(801) 378-2355 and 6536

Student Research Assistants - Charles R. Monson, Ken Bateman and Layne Pincock

Objectives

The overall objectives of this subtask are to measure and correlate fundamental reaction rate coefficients for pulverized-coal char particles as a function of char burnout in oxygen at high temperature. The effect of high pressure will be investigated.

The specific objectives for the quarterly reporting period included:

1. Continue to review appropriate literature in pertinent areas.

2. Contirue characterization of chars prepared in the HPCP from the coals selected for this study.

3. Continue oxidation tests in the HPCP reactor with chars produced from several of the coals selected for study.

Accomplishments

Three components of the subtask have been identified to accomplish the objectives outlined above: 1) design and construction of a laminar-flow, high-pressure, controlled-profile (HPCP) reactor, 2) char preparation at high temperature and high pressure, and 3) determination of the kinetics of char-oxygen reactions at high pressure.

The original program schedule called for the completion of the high-pressure char oxidation studies for pulverized coals by October, 1989. The completion date was extended with no increase in budget since the funds originally allocated for this subtask were not depleted at the end of the fourth year. The HPCP reactor, capable of functioning at 400 psi (27

atmospheres), has been constructed and instrumented to perform the fundamental reaction rate measurements required for the study. The test program was established and initiated after considerable effort to successfully complete and characterize the optical pyrometer and particle imaging system.

HPCP Reactor and Optical Instrumentation Development

The reactor is complete and was successfully operated for char oxidation experiments at up to 15 atm pressure. The particle imaging and pyrometry system was characterized and calibrated, and it has been routinely used for *in-situ* char particle temperature, velocity and size measurements.

Char Preparation at High Temperature and High Pressure

Char oxidation experiments were considered on samples selected from a set of five coals varying in rank from lignite to high-volatile bituminous: Pitt. HVA, UT Blind Canyon HVB, IL #6 HVC, Wyodak SUBC, and Beulah-Zap LIGA. These are all relatively common U.S. coals that have been used in other char oxidation studies. All of the coals are included in the Penn State, the Department of Energy and the Argonne National Laboratory coal banks. They are also standard ACERC coals.

Samples of these coals have been ground and size-classified with a combination of sieving and aerodynamic classification to produce tight size fractions of 64-74 μm and 38-44 μm. The size fractions were verified by scanning electron microscope and Coulter Counter measurements.

Chars for each of the coals have been prepared in the HPCP furnace in a nitrogen environment. All of the chars were prepared at the same reactor conditions in order to eliminate devolatilization effects on the reactivity of the chars. Char preparation conditions were as follows: atmospheric pressure, wall and gas temperatures of 1500 K, an initial particle heating rate of 10^4 (calculated using gas and wall temperature measurements), and particle residence times of 350-400 ms.

Cooperation with separately-funded researchers at BYU continued with the selection of the UT Blind Canyon HVB coal as a primary reference coal for which char will be produced in a flat-flame burner operated by another research group as well as in the HPCP for this study. Chemical and physical

property comparisons will be available to the present study in the analysis of char reactivity in the HPCP at atmospheric and elevated pressures.

Kinetics of Char-Oxygen Reactions at High Pressure

Approximately 90 char oxidation experiments have been performed with the UT Blind Canyon HVB coal chars at 1, 5, 10, and 15 atm total pressure. While it was originally planned to test with pressures up to 25 atm, it was found that high reactor temperatures could not be maintained at pressures above 15 atm. This is thought to be a result of unexpected pressure effects on the heat transfer characteristics of the furnace refractory. The UT char tests consisted of two particle size fractions (63-74 μm and 37-44 μm), reactor temperatures from 1000 to 1500 K, bulk gas O_2 concentrations from 4 to 21%, and a variety of particle residence times. This resulted in average particle temperatures ranging from 1400 to 2100 K and burnouts from 15 to 96%.

Individual particle temperature, size and velocity were determined for approximately 75 particles at each test condition. Burnouts were calculated from improved tracer measurements of ash, titanium and aluminum.

Analysis of the in-situ measurements and the collected char residues is in progress. Partial results are presented below; a detailed and complete presentation of all results will be made in the final report for this study.

Particle apparent densities were calculated from measured bulk densities, assuming an interparticle void volume of 0.45. The following correction was made for the ash content to yield the carbon apparent density, ρ_c:

$$\rho_c = \frac{1 - x_{ash}}{\frac{1}{\rho_p} - \frac{x_{ash}}{\rho_{ash}}} \qquad \text{II.B-1}$$

where ρ_p = particle apparent density

ρ_{ash} = ash apparent density (taken as 1.5 g/cc)

x_{ash} = mass fraction of ash in the sample

The change in char structure with burnout is typically modelled by the burning mode parameter, α, which is defined by the following equation:

$$\frac{\rho_c}{\rho_{co}} = \left(\frac{m}{m_o}\right)_{daf}^{\alpha} \qquad \text{II.B-2}$$

where ρ_{co} - initial carbon apparent density

m - mass of carbon

m_o - initial mass of carbon

Figure II.B-1 shows the effect of conversion on the carbon apparent density and the predicted density change from the model. The burning mode parameter most consistent with the 1 atm data, determined from least-squares regression, is 0.65, while the higher pressure data is best fit by 0.5. The 5 atm outliers at high burnout can be explained by small errors in the burnout measurements. Only a few percent increase in the burnouts brings these points into conformance with the other data. This reducing density, almost constant diameter, burning indicates that significant reaction was occurring within the particle pores (Zone I to Zone II burning). Higher total pressures did not significantly change the burning mode.

A plot of mass reactivity vs. reciprocal particle temperature is shown in Figure II.B-2. No pressure effect is apparent in the mass reactivity values. Activation energies of 20 - 25 kcal/mol best fit the data.

Plans

Samples from the 15 atm tests are yet to be analyzed, and data analysis is underway for all of the experiments in order to determine kinetic parameters at each pressure. Rather than perform only a few tests on each of four additional coal chars, it was decided to concentrate on one additional coal, Pitt. #8, of much lower reactivity than the UT coal. Approximately 16 tests will be performed at 1 and 10 atm total pressure, providing sufficient information to determine kinetic parameters.

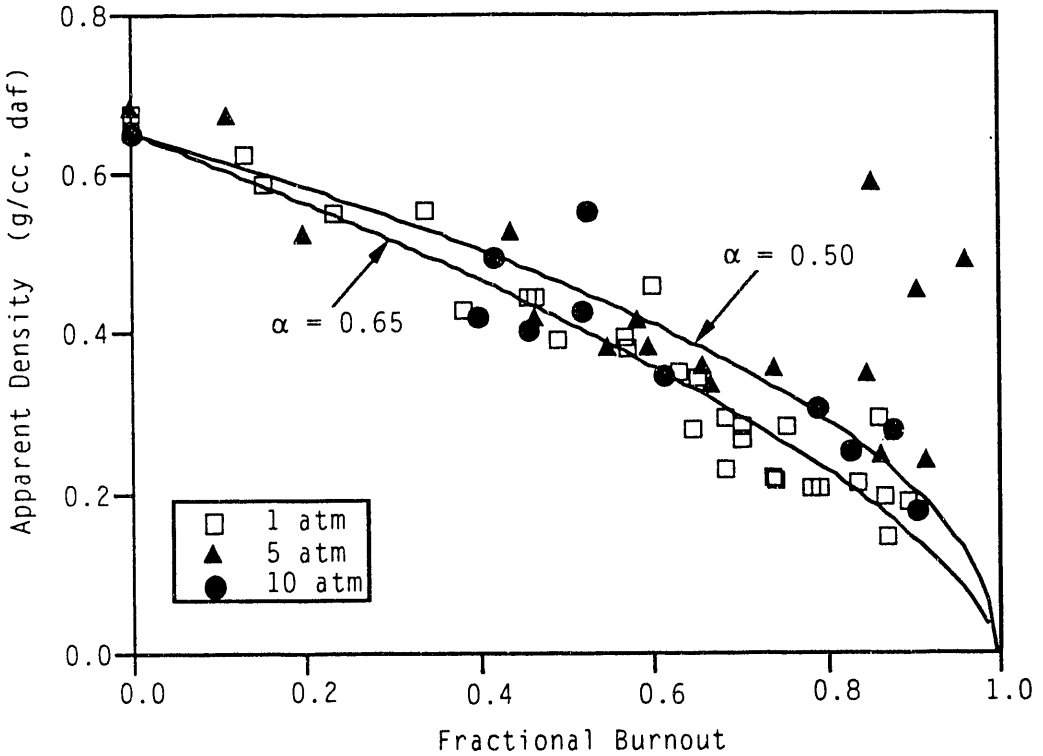

Figure II.B-1. UT Blind Canyon HVB Char Burning Mode.

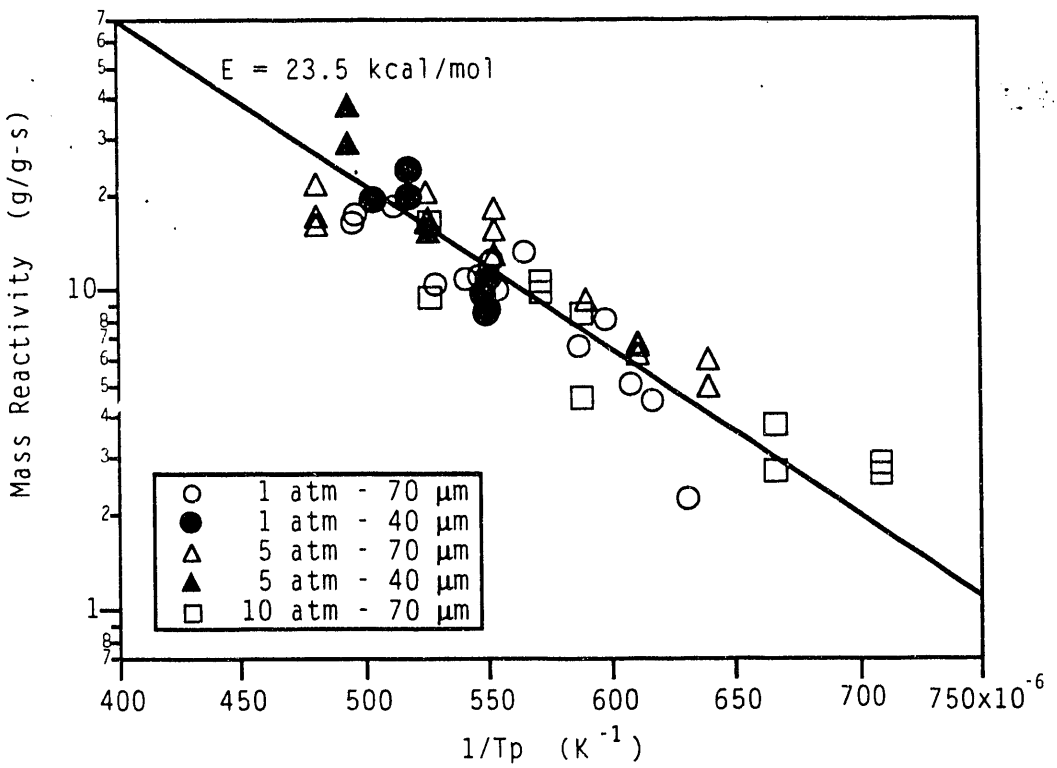

Figure II.B-2. UT Blind Canyon HVB Char Mass Reactivities.

II.C. SUBTASK 2.c. - SECONDARY REACTION OF PYROLYSIS PRODUCTS AND CHAR BURNOUT

SUBMODEL DEVELOPMENT AND EVALUATION

Senior Investigators - James R. Markham and Michael A. Serio
Advanced Fuel Research, Inc.
87 Church Street, East Hartford, CT 06108
(203) 528-9806

Objective

The objective of this subtask is to develop and evaluate by comparison with laboratory experiments, an integrated and compatible submodel to describe the secondary reactions of volatile pyrolysis products and char burnout during coal conversion processes. Experiments on tar cracking, soot formation, tar/gas reactions, char burnout, and ignition will continue during Phase II to allow validation of submodels.

Accomplishments

Discussions continued with BYU on implementation of the soot oxidation and particle ignition submodels.

Plans

Complete work with BYU on submodels for ignition and soot formation.

II.D. SUBTASK 2.d. - ASH PHYSICS AND CHEMISTRY SUBMODEL

Senior Investigator - James Markham
Advanced Fuel Research, Inc.
87 Church Street, East Hartford, CT 06108
(203) 528-9806

Objective

The objective of this task is to develop and validate, by comparison with laboratory experiments, an integrated and compatible submodel to describe the ash physics and chemistry during coal conversion processes. AFR will provide the submodel to BYU together with assistance for its implementation into the BYU PCGC-2 comprehensive code. To accomplish the overall objective, the following specific objectives are: 1) to develop an understanding of the mineral matter phase transformations during ashing and slagging in coal conversion; 2) to investigate the catalytic effect of mineral matter on coal conversion processes.

Accomplishments

No work scheduled.

Plans

Complete work on submodel for ash chemistry and physics.

II.E. SUBTASK 2.e. - LARGE PARTICLE/THICK BED SUBMODELS

Senior Investigator - Michael A. Serio
Advanced Fuel Research, Inc.
87 Church Street
East Hartford, CT 06108
(203) 528-9806

Objective

The objectives of this task are to develop or adapt advanced physics and chemistry submodels for the reactions of "large" coal particles (i.e., particles with significant heat and/or mass transport limitations) as well as thick beds (multiple particle layers) and to validate the submodels by comparison with laboratory scale experiments. The result will be coal chemistry and physics submodels which can be integrated into the fixed-bed (or moving-bed) gasifier code to be developed by BYU in Subtask 3.b. Consequently, this task will be closely coordinated with Subtask 3.b.

Accomplishments

Work continued on exploring the reduced tar yields in high pressure gasifiers. In the previous quarterly, laboratory studies showed no evidence of tar gasification by CO_2 at temperatures between 800 and 1000 °C. However, significant tar cracking occured during post-pyrolysis in helium at similar temperatures, resulting in the formation of light hydrocarbon gases (CH_4, C_2H_4, C_2H_2, ..., etc.). In order to confirm this conclusion, the compositions of products from high pressure and atmospheric gasifiers were compared.

For a fair comparison, mass balance calculations using data in an EPRI report (GS-6797, Oct., 1990) were done on a high pressure (300 psig, GE) and an atmospheric (MIFGa/USBM) gasifiers, both of which used Illinois coal as feedstock and were operated at similar coal and air input rates for several runs, although the high pressure gasifier had a higher steam input.

The high pressure gasifier, which had a low tar yield, had a longer gas phase residence time, and increased yields of dust and CH_4. The average yields of tars, CH_4 and dust were compared. Interestingly enough, the total yields of tar, dust and CH_4 are close for the two different gasifiers. Consequently, it can be concluded that tar thermal cracking to form hydrocarbon light gases and dust (or soot) is primarily responsible for the low tar yields observed from the high pressure gasifiers.

Modeling of Tar Destruction in a Moving-Bed Gasifier

Work continued on exploring the reduced tar yields in high pressure gasifiers. In the previous quarterly, laboratory studies showed no evidence of tar gasification by CO_2 at temperatures between 800 and 1000 °C. However, significant tar cracking occured during post-pyrolysis in helium at similar temperatures, resulting in the formation of light hydrocarbon gases (CH_4, C_2H_4, C_2H_2, ..., etc.). Although post-pyrolysis of tars in the presence of steam was not studied, it has been reported that tar yields in pyrolysis increased with the presence of steam, possibly since steam could occupy char active sites which cause the cracking of tars (Dryden and Sparham, 1963). Consequently, it was concluded that the tar destruction in the top part of a fixed-bed gasifier can probably be attributed primarily to thermal cracking rather than gasification reactions. In order to confirm this conclusion, the compositions of products from high pressure and atmospheric gasifiers were compared.

For a fair comparison, mass balance calculations using data in an EPRI report (GS-6797, Oct., 1990) were done on a high pressure (300 psig, GE) and an atmospheric (MIFGa/USBM) gasifiers, both of which used Illinois coal as feedstock and were operated at similar coal and air input rates for several runs, although the high pressure gasifier had a higher steam input. The input and output data for those runs are shown in Table II.E-1.

As shown in Table II.E-1, the average inputs of coal and air for both of the gasifiers were approximately 1800 lb/hr and 4400 lb/hr, respectively. The average tar output was much lower for the higher pressure gasifer than the atmospheric one, while the total yield of dry gases was higher for the high pressure gasifier than the atmospheric one. The data for dry gas and tar analyses are shown in Table II.E-2. One can see that the output rates of CO_2 and H_2 were higher, while that of CO was lower,

Table II.E-1 The Input and Output Rates in Pressurized and Atmospheric Moving-Bed Gasification of Illinois #6 Coal

Inputs (lb/hr)				Outputs (lb/hr)				
Test No.	Coal	Steam	Air	Dry Gas	Water	Tar	Dust	Ash
300psig								
401	1858	1728	4309	6348	1062	52.4	97.2	190.7
403	1627	2581	4348	6404	1757	70.7	51.8	150.3
404	1813	1717	4343	6448	983	53.2	34.2	219.6
406	1848	1742	4308	6517	1179	76.5	23.2	209.7
407	1963	1728	4345	6729	1028	87.0	61.4	202.6
Average	1822	1899	4331	6489	1202	68.0	52.7	194.6
14.7psig								
007-01	1640	998	4638	6090	761	123	6	227
007-02	2025	948	4745	6471	747	272	8	259
007-03	2036	875	4714	6427	704	269	8	228
007-04	2042	777	4718	6357	638	287	8	270
007-08	1568	677	4117	5409	636	195	5	219
007-09	1579	631	3970	5204	574	229	5	199
Average	1815	818	4484	5993	677	229	6.7	234

Table II.E-2 Dry Gas and Tar Analysis in Pressurized and Atmospheric Moving-Bed Gasification of Illinois #6 Coal

Dry Gas Analysis (vol %)							Tar Analysis (wt %)					
Test No.	CO	CO_2	H_2	CH_4	N_2	Ar	Ash	C	H	N	S	O
300psig												
401	16.53	12.42	20.93	4.23	45.07	0.50	5.44	82.05	5.73	1.12	2.28	3.38
403	9.85	17.11	21.61	4.55	46.12	0.50	5.44	82.05	5.73	1.12	2.28	3.38
404	18.32	11.41	20.42	4.40	44.65	0.50	5.44	82.05	5.73	1.12	2.28	3.38
406	18.50	11.50	21.50	4.29	43.41	0.50	5.44	82.05	5.73	1.12	2.28	3.38
407	17.96	12.90	20.92	4.49	42.99	0.50	5.44	82.05	5.73	1.12	2.28	3.38
Average	16.23	13.07	21.08	4.39	44.45	0.50	5.44	82.05	5.73	1.12	2.28	3.38
Average(wt %)	18.88	23.90	1.75	2.92	51.72	0.83						
Average Flow Rate(lb/hr)	1225	1551	113.60	189.50	3356	53.93						
14.7psig												
007-01	19.71	9.44	15.93	1.35	51.77	0.62	0.10	81.37	7.03	1.17	2.44	7.88
007-02	22.80	7.85	17.37	1.44	48.65	0.58	0.10	81.37	7.03	1.17	2.44	7.88
007-03	23.99	7.08	16.68	1.63	48.73	0.58	0.10	81.37	7.03	1.17	2.44	7.88
007-04	24.55	6.41	15.97	1.73	49.44	0.59	0.10	81.37	7.03	1.17	2.44	7.88
007-08	21.35	8.41	14.88	1.54	51.95	0.62	0.10	81.37	7.03	1.17	2.44	7.88
007-09	22.24	7.43	15.62	1.50	51.35	0.61	0.10	81.37	7.03	1.17	2.44	7.88
Average	22.44	7.77	16.08	1.53	50.32	0.60	0.10	81.37	7.03	1.17	2.44	7.88
Average(wt %)	25.54	13.90	1.31	0.99	57.28	0.97						
Average Flow Rate(lb/hr)	1531	883	78.5	59.64	3433	58.47						

for the high pressure gasifier. This is probably due to the contribution of the water-gas shift reaction

$$CO + H_2O \rightleftarrows CO_2 + H_2$$

in the gasifiers, since the pressure of steam was higher in the high pressure gasifier. The output rates on a molar basis for CO, CO_2 and H_2 are shown in Table II.E-3. The data suggest that the water-gas shift reaction accounts for the most of the higher CO_2 and H_2 and lower CO yields in the high pressure gasifier.

The dry gas analysis in Table II.E-2 shows higher yields of CH_4 for the high pressure gasifier. The concentrations of other light hydrocarbons were low compared to CH_4, and are not shown in the EPRI report. The high CH_4 yield suggests that enhanced cracking of tars occurs in the high pressure gasifier to form additional hydrocarbon light gases. The residence time of tars in the gasifier may be the major factor affecting the amount of tar cracking. The volumetric output rate of dry gases in the high pressure gasifier was only 1.2 times higher than that in the atmospheric one, while the pressure is 21 times higher, indicating the residence time in gas phase was much longer for the high pressure gasifier.

Significant differences between tars from the high pressure and atmospheric pressure gasifiers can be seen in the tar analyses shown in Table II.E-2. The higher ash content in tars from the high pressure gasifier suggests significant secondary cracking of the organic portion. The hydrogen and oxygen contents were also lower for tars from the high pressure gasifier, suggesting more severe secondary pyrolysis of tars in this system. These differences in tar composition can be attributed to the longer residence time in the high pressure gasifier.

It can be noted from Table II.E-1 that the yield of dust was much higher for the high pressure gasifier. The ash contents of the dusts were 8.5 wt% for the high pressure gasifier and 21 wt% for the atmospheric one. The composition of the dust from the high pressure gasifier on an ash-free basis indicates a high carbon content and low hydrogen content which is consistent with the composition of soot formed from tar cracking.

Table II.E-3 Comparison of Yields of CO, CO_2 and H_2 for the High Pressure and Atmospheric Pressure Gasifiers

Gasifier	Flow Rate (lbmol/hr)		
	CO	CO_2	H_2
300 psig	43.8	35.3	56.8
1 atm	54.7	20.0	39.3
Difference	-10.9	15.3	17.5

Table II.E-4. Mass Balance on Tar, Dust and CH_4 for the Gasifiers

Gasifier	Flow Rate (lb/hr)			
	Tar*	CH_4	Dust*	Sum
300 psig	64	190	48	302
1 atm	229	60	5.3	294

* Ash excluded

The high pressure gasifier, which had a low tar yield, had a longer gas phase residence time, and increased yields of dust and CH_4. The average yields of tars, CH_4 and dust are compared in Table II.E-4. Interestingly enough, the total yields of tar, dust and CH_4 are close for the two different gasifiers. Consequently, it can be concluded that tar thermal cracking to form hydrocarbon light gases and dust (or soot) is primarily responsible for the low tar yields observed from the high pressure gasifiers.

Plans

Complete development of tar destruction submodel. Complete development of single particle model with BYU.

II.F. SUBTASK 2.F. - LARGE PARTICLE OXIDATION AT HIGH PRESSURES

Senior Investigators: Angus U. Blackham and Geoffrey J. Germane
Brigham Young University
Provo, Utah 84602
(801) 378-2355 and 6536
Student Research Assistants: Ken Bateman and Parvin Yousefi

Objectives

The overall objective for this subtask is to provide data for the reaction rates of large char particles of interest to fixed-bed coal gasification and combustion systems operating at pressure.

The specific objectives for this quarter include:

1. Continue the construction of the cantilever beam balance unit.

2. Conduct additional preliminary oxidation experiments.

Accomplishments

The two components of this subtask that have been suggested earlier for accomplishing the overall objective are: 1) reactor design, fabrication, and preliminary data; 2) experimental reaction rate data for chars from five coals. Construction of a cantilever beam balance unit to be connected to an optical access port of the HPCP reactor has continued during this quarter.

The data previously presented as preliminary oxidation measurements of large char particles of six different coals have been organized into a manuscript and submitted for publication. A thick-ash-layer theory was developed and was supported by the experimental observation that the cube root of the char particle mass declined linearly with time in all tests of the 35 particles. Average mass reactivities were correlated with initial char particle mass, temperature, and ash fraction.

An additional 70 tests have been performed during this quarter in order to extend the temperature range and also focus on the final 20-30 percent of burnout. These data are being studied in light of the thick-ash-layer theory referred to above.

Reactor Design

Cantilever Beam Balance Unit - The cantilever beam balance unit was designed to give mass loss readings and to precisely locate the sample during oxidation experiments using 0.5-1.0 cm char particles. The three components of the cantilever beam balance unit are: a) a balance unit; b) a three-axis slide; and c) a heat-shielded, water-cooled valve. The entire assembly will be bolted directly to the HPCP reactor of Subtask 2b.

The balance unit measures the mass loss of the particles as they oxidize in the HPCP reactor. It consists of a force transducer, a ceramic cantilever beam and a platinum wire-mesh sample basket. The basket is secured to the cantilever beam and extends into the reactor tube through one of the optical access ports of the HPCP reactor.

In order to test multiple samples during each run, a mechanism has been designed to insert and retract the samples from the reactor tube. The balance unit is mounted on a mobile platform. The slide has been improved to include movement along three axes. With this improvement the particle can be moved in all directions while being oxidized. First, the entire unit will move toward and away from the reactor tube in the horizontal direction by way of a stepper motor. The remaining two directions will be performed by way of a manual positioner. The positioners will allow for 10 mm of movement. Construction of the main components of the three-axis slide has been completed. Assembly of the components is almost completed. The high-pressure shell to house the slide assembly is almost completed. These features are shown in Figure II.F-1 and Figure II.F-2.

Oxidation Measurements

Preliminary Large-Particle Oxidation Measurements - The data previously presented (Solomon, et.al, 1990,1991,1992) as preliminary oxidation measurements of large char particles in platinum crucibles by convective air flow heated in a muffle furnace or with a Meker burner have been organized into a manuscript and submitted for publication. Both a thin- and thick-ash-layer theory were developed and tested with these data from the oxidation of 35 char particles in which six different coals were represented. Test variables were coal type, oxidation temperature, and initial char particle mass. The cube root of particle mass declined linearly with time in all

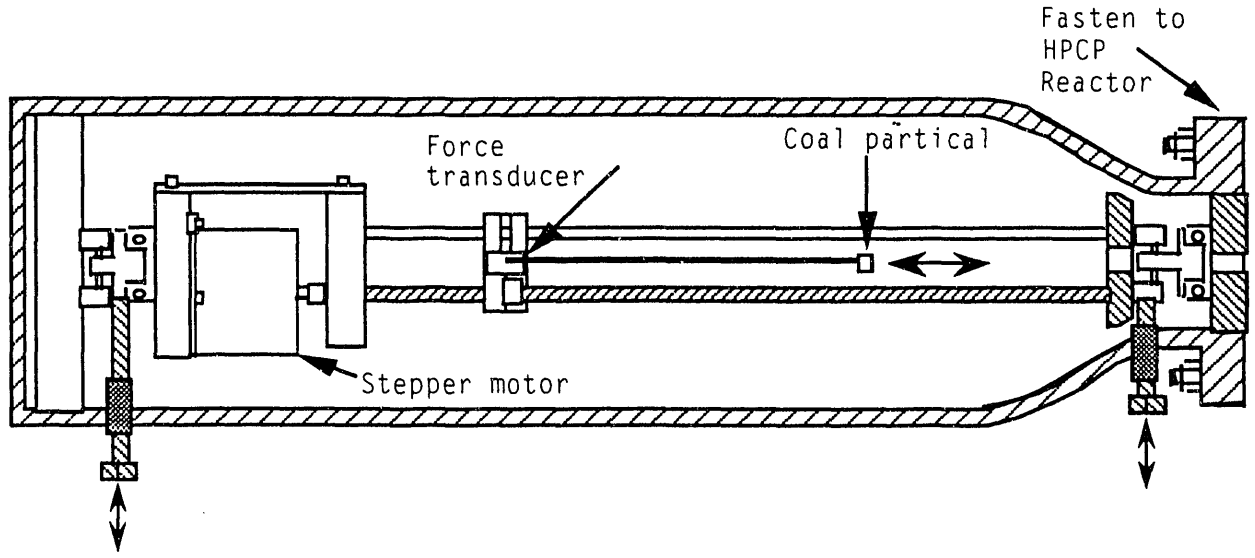

Figure II.F-1. Three-axis slide assembly.

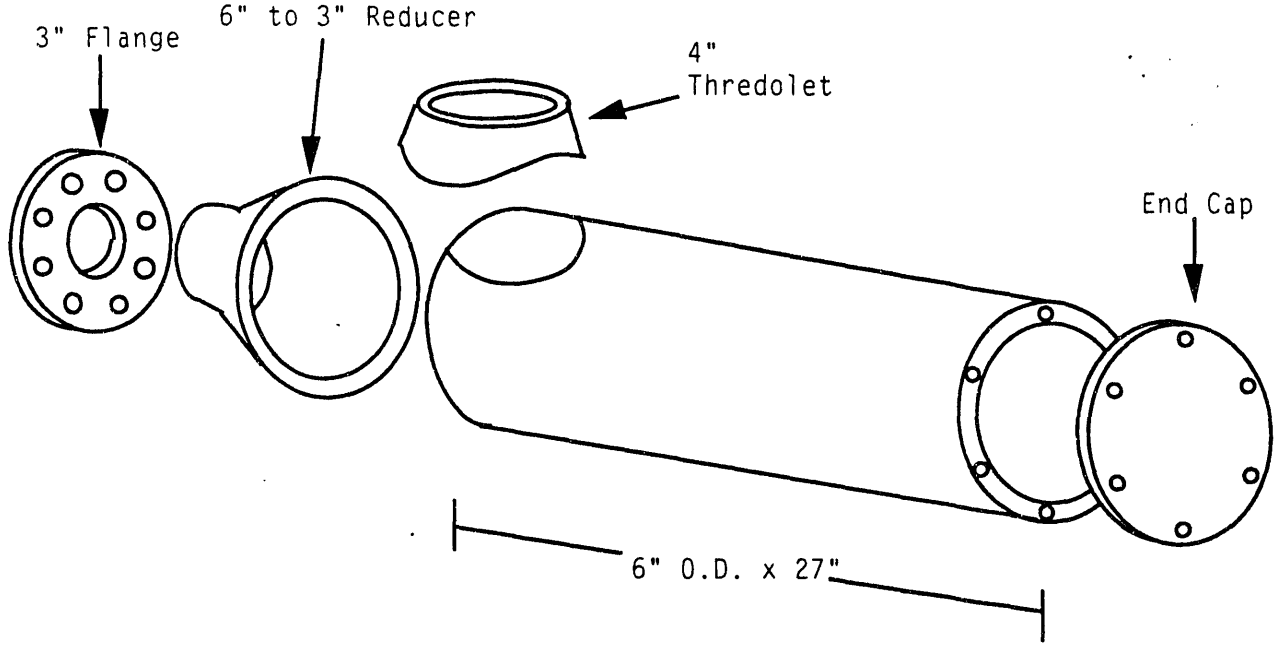

Figure II.F-2. High-pressure shell to house slide assembly.

tests, which supported the thick-ash-layer theory. Ash layers formed and usually remained in place around the char particles. Average mass reactivities increased with decreasing initial char particle mass and possibly with decreasing char ash percentage. Increasing furnace temperature had little impact on char reactivity. Correlations of average mass reactivity were presented in the 22nd Quarterly Report (Solomon et al., 1992). The observations are consistent with oxidation being controlled by diffusion of oxygen through the ash layer.

About forty additional tests have been made. These data have been graphed and are being studied in light of the theories considered earlier. Interpretations will be made and included in the final report. Some comparisons of coal and char properties have been made on the four coals used for these additional tests. For the Colorado bituminous coal, the devolatilization step is rather short (2 minutes). Only small traces of tar are produced. The particle does not swell after this step. The ash formed during oxidation usually does not flake away and keeps the original shape of the char particle. The ash color is red. The Illinois 6 bituminous coal takes a longer time to devolatilize (3-4 minutes). The particle size almost doubles. The ash usually keeps the original shape of the particle. However, in some cases, the ash breaks down after about 70% of the oxidation period. The ash color is orange and gray. The North Dakota lignite takes about 2 minutes to devolatilize but some oxidation is also evident during this period and it takes a longer time for the particle to cool. The ash layer usually remains intact during the oxidation. The ash color is white. The Utah bituminous coal swells during the devolatilization step and sometimes cracks and breaks down before the oxidation is completed. However, some of the Utah char samples have kept the original shape up to the end of oxiation. The ash color is orange.

Plans

During the next quarter the construction of the cantilever beam balance unit will be completed and tested for its accuracy and reproducibility in positioning the sample char particle in the reactor. The rates of oxidation of the selected coals will then be made at pressures above atmospheric.

Additional preliminary oxidation runs will be made in air in platinum crucibles to resolve some of the issues raised with the previous preliminary experiments.

II.G. SUBTASK 2.G. - SO_x/NO_x SUBMODEL DEVELOPMENT

Senior Investigators: L. Douglas Smoot and B. Scott Brewster
Brigham Young University
Provo, Utah 84602
(801) 378-4326 and (801) 378-6240

Research Assistant: Richard D. Boardman

Objectives

The objectives of this subtask are 1) to extend an existing pollutant submodel in PCGC-2 for predicting NO_x formation and destruction to include thermal NO, 2) to extend the submodel to include SO_x reactions and SO_x-sorbent reactions, and 3) to consider the effects of fuel-rich conditions and high pressure on sulfur and nitrogen chemistry in pulverized-fuel systems.

Accomplishments

The option for capturing H_2S was tested by simulating the BYU gasifier with and without sorbent injection. The test conditions corresponded to Test No. I9, Sample No.3 (without sorbent injection) and Test No. I10, Sample No. 4 (with sorbent injection) in Table II.H-2 of the 3rd Annual Report (Solomon et al., 1989). Results are shown in a paper that was prepared for the 1992 International Joint Power Generation Conference, sponsored by The American Society of Mechanical Engineers and to be held in Atlanta, Georgia on October 18-22, 1992. The paper was accepted, and a copy is included in the appendix.

The degree of sulfur capture is over-predicted, presumably because the 2-D simulation is incapable of adequately representing the 3-D mixing effects of cross-flow injection from the sidewall. This shortcoming is discussed in the paper. Other limitations of the submodel include: 1) H_2S and SO_2 cannot be captured simultaneously. The sorbent particle sulfation submodel cannot deal with the simultaneous formation of $CaSO_4$ and CaS. 2) No conversion of H_2S to SO_2 is allowed once it is formed, and visa versa. There is no homogeneous chemistry included in the submodel. 3) Sulfur is released from the coal at a rate which is proportional to its total weight loss, and SO_2 and H_2S are formed in a ratio equal to that of the reactor exit gas without

sorbent injection. The FG-DVC submodel predicts the rate of sulfur release. However, this information was not used in this first version of a sorbent reactions submodel because the limitations imposed by the lack of homogeneous chemistry are deemed to be more restrictive by comparison. Since there is no interconversion among sulfur species once they are formed, SO_2 and H_2S must be formed initially in the same ratio which would exist in the product gas without sorbent injection.

Although this first version of a sorbent reactions submodel has some rather restrictive limitations, it has demonstrated the feasibility of using the shrinking-core grain model of Silcox (1985) and Silcox et al. (1989) to predict sorbent particle reactions in a comprehensive code. Future enhancements should address such questions as the effects of sorbent particle calcination kinetics, interconversion of sulfur species in the gas phase, evolution of sulfur from the coal at a rate predicted by FG-DVC, and simultaneous capture of SO_2 and H_2S.

Plans

This subtask is complete. No further work is planned.

SECTION III. TASK 3. COMPREHENSIVE MODEL DEVELOPMENT AND EVALUATION

Objectives

The objective of this task is to integrate advanced chemistry and physics submodels into a comprehensive two-dimensional model of entrained-flow reactors (PCGC-2) and to evaluate the model by comparing with data from well-documented experiments. Approaches for the comprehensive modeling of fixed-bed reactors will also be reviewed and evaluated and an initial framework for a comprehensive fixed-bed code will be employed after submission of a detailed test plan (Subtask 3.b).

Task Outline

This task is being performed in three subtasks. The first covers the full 72 months of the program and is devoted to the development of the entrained-bed code. The second subtask is for fixed-bed reactors and is divided into two parts. The first part (12 months) was devoted to reviewing the state-of-the-art in fixed-bed reactors. This led to the development of the research plan for fixed-bed reactors, which was approved. The code development is being done in the remaining 60 months of the program. The third subtask is to generalize the entrained-bed code to fuels other than dry pulverized coal and will be performed during the last 36 months of the program.

III.A. SUBTASK 3.A. - INTEGRATION OF ADVANCED SUBMODELS INTO ENTRAINED-FLOW CODE, WITH EVALUATION AND DOCUMENTATION

Senior Investigators - B. Scott Brewster and L. Douglas Smoot
Brigham Young University
Provo, UT 84602
(801) 378-6240 and 4326

Research Assistants - Ziaul Huque and Susana K. Berrondo

Objectives

The objectives of this subtask are 1) to integrate the FG-DVC submodel into PCGC-2, 2) incorporate additional submodels and improvements developed under Task 2, 3) evaluate the improved code, 4) improve user-friendliness and robustness, and 5) document the code.

Accomplishments

Submodel Integration

A new equilibrium algorithm was integrated into PCGC-2 during the past quarter and is being tested. The new algorithm is based on the METCEC code (Nicoletti, 1986a, 1986b) that was obtained with the help of Dr. Thomas J. O'Brien at METC. The new algorithm is similar to the CREE algorithm that existed previously in PCGC-2, but it allows for condensed phases. It was developed from the well-known NASA-Lewis equilibrium code that also formed the basis of CREE. The CREE routine was retained in PCGC-2 and modified to work with the new routines taken from METCEC, which consist of a routine named SPECE and all of the routines that it calls. The old algorithm also had a routine named SPECE, so the integration mainly consisted of replacing the old SPECE with the new SPECE and adding all the new routines which it calls. The new algorithm was shown to correctly predict chemical equilibrium with solid carbon for a test case that previously failed with the old algorithm. It is hoped that the new algorithm will bring the predicted gas composition in PCGC-2 into agreement with the equilibrium constant of the water-gas-shift reaction, which is the anomaly that uncovered the problems with the old algorithm.

Code Evaluation

The code is being evaluated by comparison with data from five reactors: the AFR transparent wall reactor (TWR), the BYU/ACERC controlled-profile reactor (CPR), the Imperial College reactor, the BYU gasifier, and the Combustion Engineering (CE) drop-tube furnace. Calculations were performed during the past quarter for the CPR and Imperial College reactor. In addition, a problem with the gas-particle momentum coupling was uncovered and corrected.

BYU/ACERC Controlled-Profile Reactor (CPR) - A diagram of the CPR and results of gas flame simulations were given in the 5th Annual Report (Solomon et al., 1991). Input conditions and predictions for coal combustion were given in the 21st Quarterly Report (Solomon et al., 1991). These predictions were made using a swirl no. of 0.8 rather than the reported value of 1.4, consistent with the recommendations of Harding (1980) for theoretical and measured swirl numbers. Use of the reported swirl no. resulted in the particles travelling along the front wall of the reactor due to an incorrectly predicted external recirculation zone. In the 22nd Quarterly Report (Solomon et al., 1992), it was reported that the external recirculation zone could be predicted reasonably well at the reported value of swirl no. (1.4) if a finer grid were used. During the last quarter, two cases of coal combustion in the BYU controlled-profile reactor were simulated using the latest version of the FG-DVC submodel. Comparisons of predictions with temperature data were performed. Comparison with the species concentration data will be performed when the data are available.

Imperial College Reactor - A description of available data sets for the axisymmetric, Imperial College reactor was given in the 5th Annual Report (Solomon et al., 1991). A schematic diagram of the reactor was shown in the 21st Quarterly Report (Solomon et al., 1991). In the 5th Annual Report, it was reported that the directions of both the internal and external recirculation zones are incorrectly predicted. No flow reversal was seen on the centerline near the inlet. In the 21st Quarterly Report, the effects of swirl no. were investigated, but flow reversal on the centerline was not predicted. Flow reversal was predicted at swirl nos. greater than approximately 0.35 by use of a finer grid, as reported in the 22nd Quarterly (Solomon et al., 1992).

During the last quarter, two of the six cases, namely Cases A and F (see Table III.A-2, 5th Annual Report), were simulated using the latest version of FG-DVC in PCGC-2. It was observed that correct prediction of the external recirculation zone (ERZ) and the internal recirculation zone (IRZ) depend on the size of the inlet quarl geometry for cases where the swirl number is above a critical value. The critical swirl number is defined as that value above which the flow reverses its direction in the central region. For reactors with no inlet quarl or small inlet quarl dimensions (e.g. the Imperial College reactor) and with swirl number above the critical value, the IRZ is overpredicted in size, and the ERZ is either too small or totally absent. In order to reduce the overprediction of the IRZ, both cases were simulated with swirl nos. equal to about half the reported values. Simulation results for Case A are shown below.

Predicted velocity vectors and particle trajectories are shown in Figure III.A-1. Some of the larger particles do not experience a reversal in axial direction. The maximum penetration of the particles which experience a reversal in direction is about 0.6 m. After reversal, the particles flow along the side wall, suggesting that the ERZ is still not predicted correctly. Figure III.A-2 gives the plots for one representative particle trajectory. The burnout for this trajectory was complete at about 1.2 m from the inlet. The maximum particle temperature attained was about 1250 K. Figures III.A-3 and III.A-4 show the comparisons of the predicted radial oxygen concentration and temperature profiles with experimental data at several axial locations. Predicted trends of radial oxygen concentration profiles are found to reproduce the observed trends except at locations nearest the burner. The radial temperature profiles are found to be in good agreement near the side wall, but temperature is underpredicted near the centerline up to an axial distance of 0.5 m. The low temperature is due to the scarcity of oxygen in that region as shown in Figure III.A-3. The incoming, oxygen-containing stream gets diverted and flows along the wall. According to Figure III.A-3, oxygen gets properly mixed and the oxygen profile is correctly predicted at an axial distance of about 0.72 m. Temperature profiles are also expected to be predicted correctly at this location, but there are no experimental data with which to compare.

Particle Momentum Coupling - A problem with the gas-particle momentum coupling was uncovered by independent work performed under a DOE-sponsored Phase II SBIR program (Grant No. DE-FG05-90ER80877), where PCGC-2 is

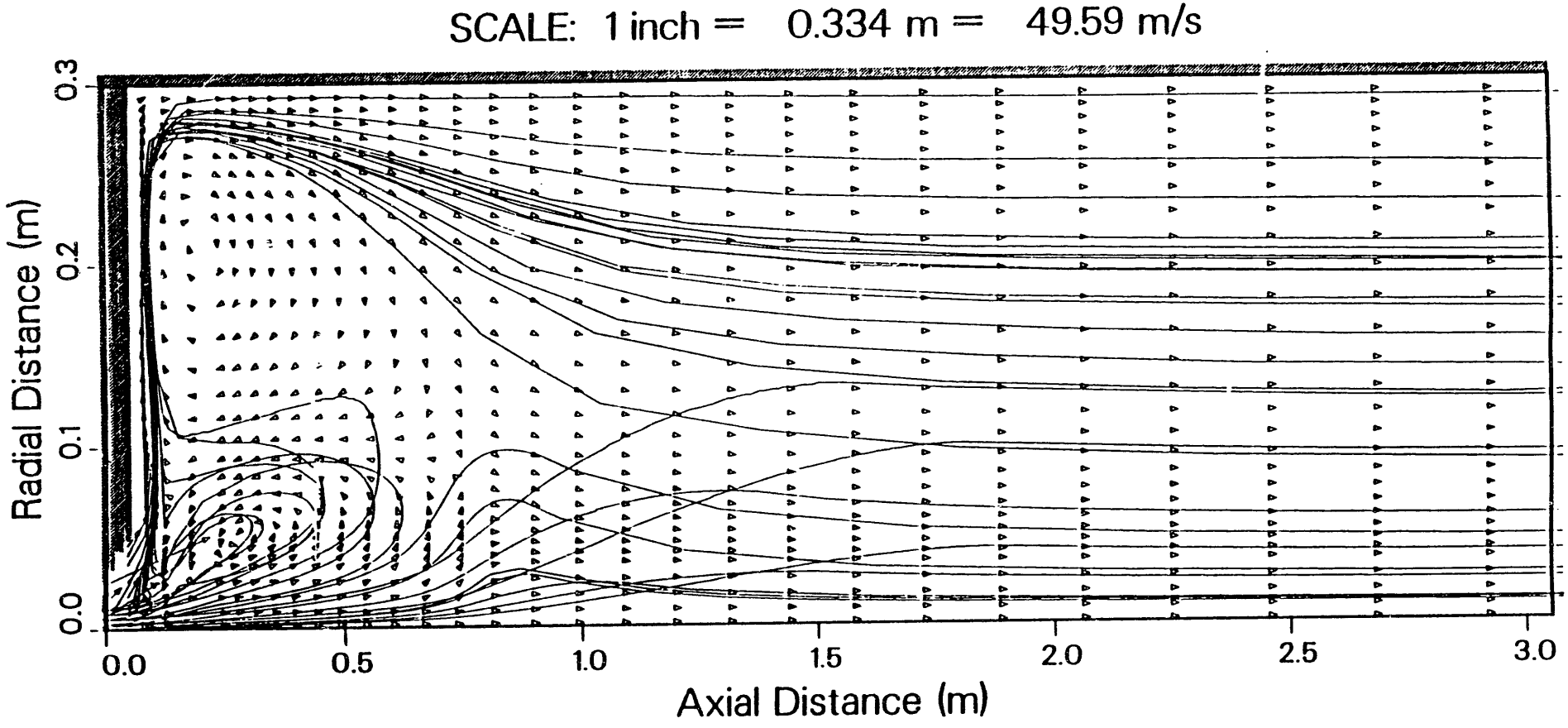

Figure III.A-1. Predicted velocity vectors and particle trajectories for Imperial College case A coal combustion using UK Geddling bituminous coal with a secondary swirl nmber of 0.78

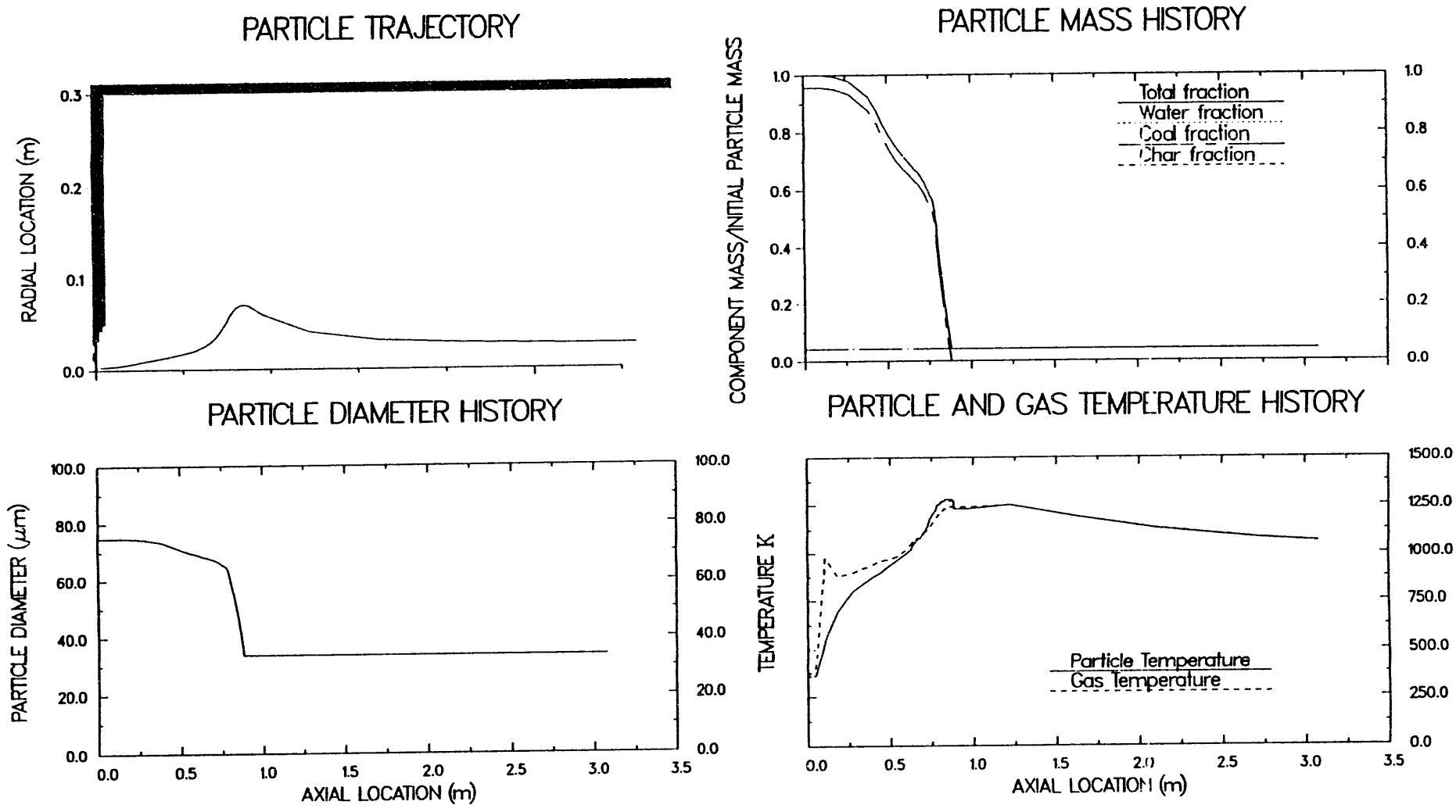

Figure III.A-2. Trajectory, mass, diameter and temperature history for 75 μm size particle from one starting location for Imperial College coal combustion case A using UK Geddling bituminous coal.

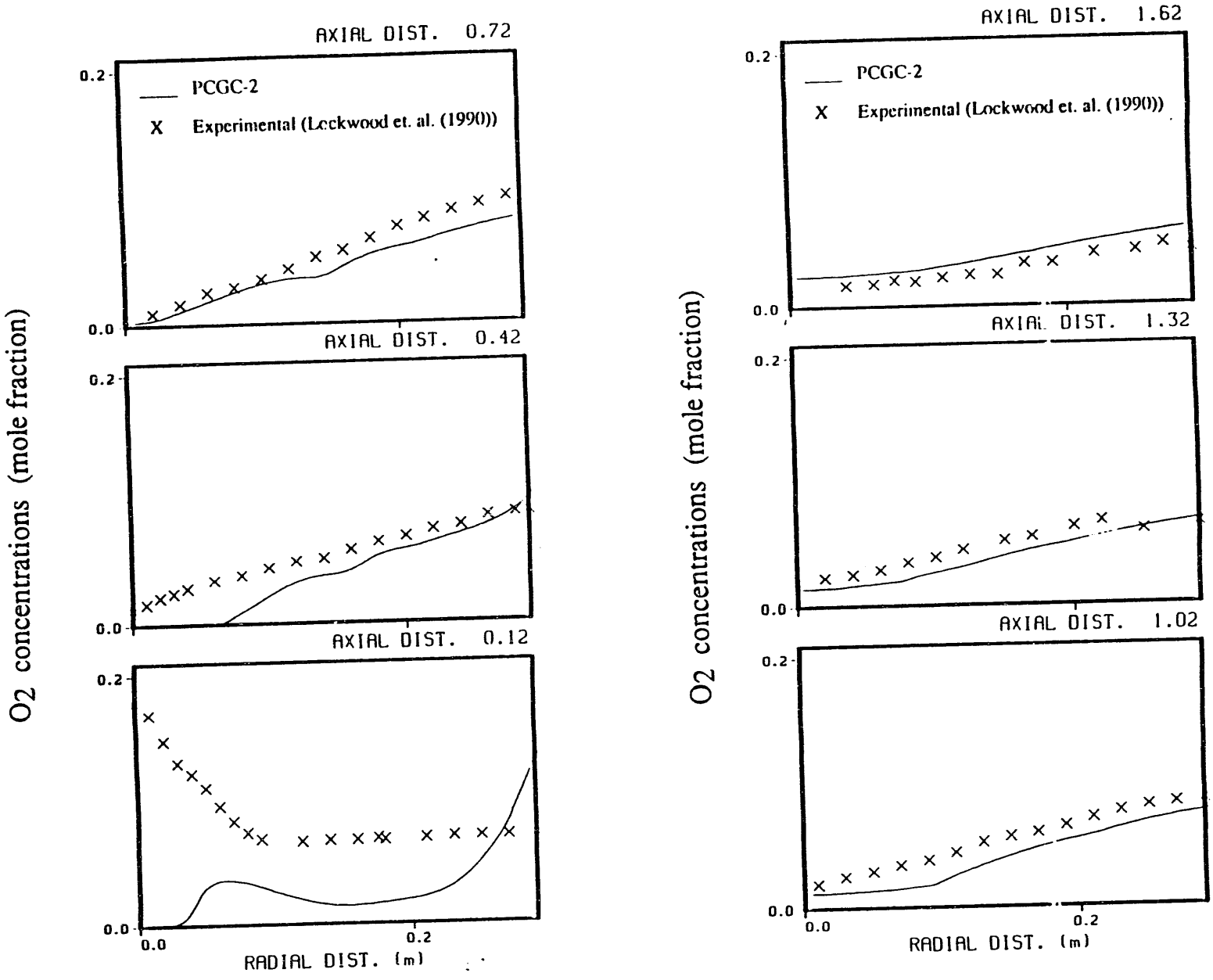

Figure III.A-3. Comparison of predicted radial O_2 concentration profiles with experimental data for Imperial College coal combustion case A with secondary swirl number of 0.78.

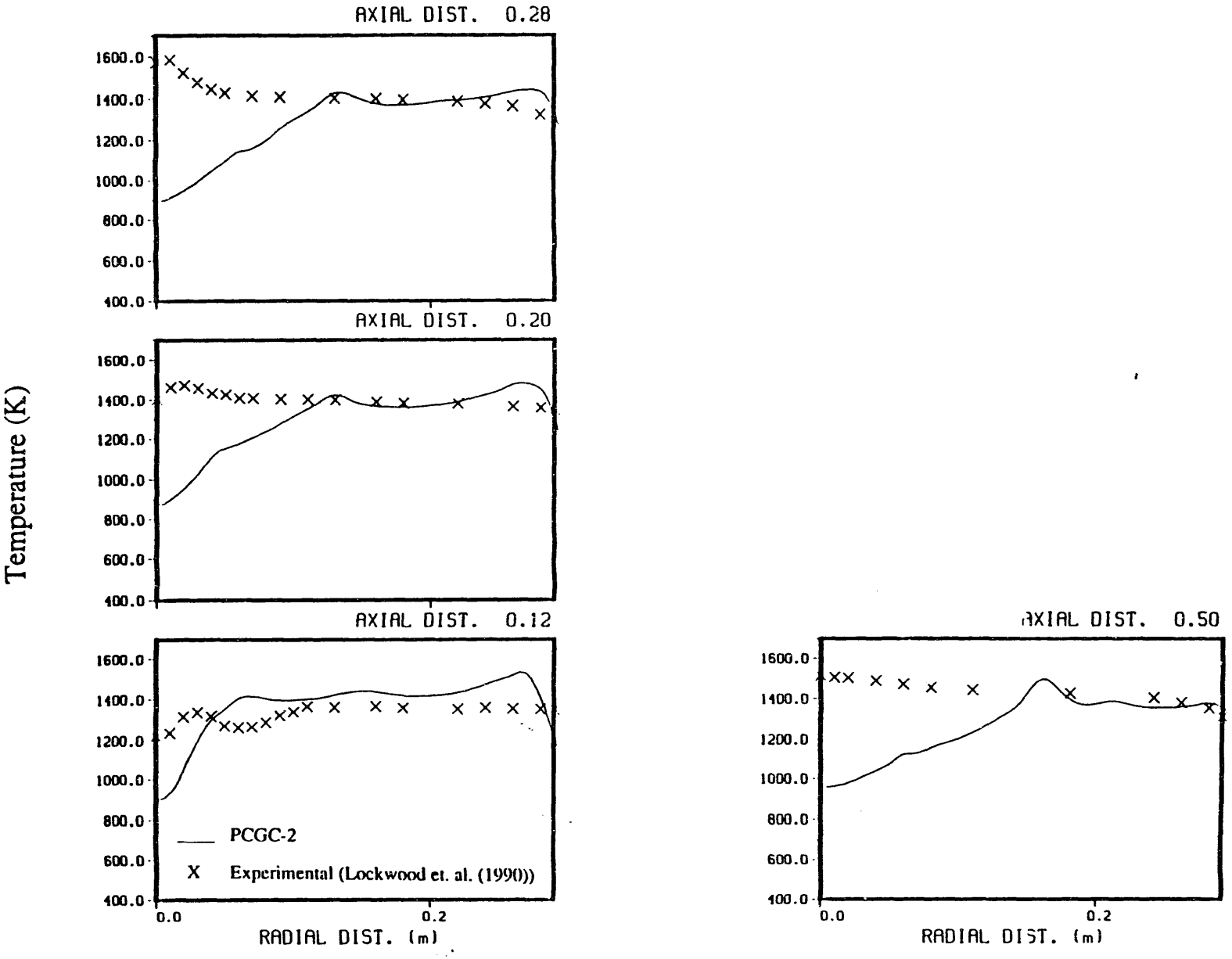

Figure III.A-4. Comparison of predicted radial temperature profiles with experimental data for Imperial College coal combustion case A with secondary swirl number of 0.78.

being modified by AFR and applied to mild gasification in a transport reactor. The problem became apparent in the densely-loaded system of the transport reactor, where the momentum coupling term in dominant. The problem was that the entire change in particle momentum in a computational cell was being attributed to interaction with the gas, in agreement with the original paper on the particle-source-in-cell (PSI-CELL) technique published by Crowe et al. (1977). However, changes in particle momentum due to gravitational forces should not be attributed to the gas; only the drag effects in the particle momentum equation in PCGC-2 should be included in the momentum coupling with the gas. This conclusion was confirmed through a telephone call to Clayton Crowe, and his suggestion for splitting the drag term into two parts, an "S_p" term that gets multiplied by the gas velocity and which is always negative (for stability in the SIMPLE algorithm used in PCGC-2) and an "S_u" term that contains the rest of the momentum coupling, were implemented in PCGC-2.

Plans

Work on code development and evaluation is nearly complete. Code graphics development is nearly complete. Preparation of the user's manual has been initiated. During the next quarter, code graphics and the user's manual will be completed.

III.B. SUBTASK 3.B. - COMPREHENSIVE FIXED-BED MODELING REVIEW, DEVELOPMENT, EVALUATION, AND IMPLEMENTATION

Senior Investigators - Predrag T. Radulovic and L. Douglas Smoot
Brigham Young University
Provo, Utah 84602
(801) 378-3097 and (801) 378-4326

Research Assistant - M. Usman Ghani

Objectives

The objectives of this subtask are: 1) to develop an advanced fixed-bed model incorporating the advanced submodels being developed under Task 2, particularly the large-particle submodel (Subtask 2.e.), and 2) to evaluate the advanced model.

Accomplishments

During the last quarter, work continued on developing and evaluating the fixed-bed model, FBED-1. The consolidation of data for the final simulations of a high pressure, Lurgi gasifier and an atmospheric pressure Wellman-Galusha gasifier was completed. The problem of extremely steep temperature gradients and devolatilization rates was resolved by properly modeling the energy exchange effects between the solid and the gas phases. An option to allow the thermal decomposition of tar in the gas phase was added. Major modifications in the code were made to improve the code structure and enhance user friendliness. Options were added in the fixed-bed code to choose among various devolatilization submodels, e.g., FG-DVC and FG-SET with variable number of functional groups. Work on improving the zero-dimensional portion of the code was initiated. A paper on fixed-bed modeling was published (Hobbs et al., 1992).

Data Consolidation

The consolidation of data for the final simulations of a high pressure, Lurgi gasifier and an atmospheric pressure Wellman-Galusha gasifier was completed. The subprogram, ADJSTYO, to adjust the starting functional group composition of coal to match its ultimate composition was rewritten to

accommodate the additional functional groups. An additional subprogram was incorporated in the code to select the appropriate data file for the coal dependent parameters for the devolatilization submodel. Eight data files for the standard (Argonne premium) coals are provided. Three options are included. The first option allows the program to select the standard coal which is closest, on a oxygen/carbon-hydrogen/carbon plot, to the feed coal. The second option allows the user to specify a standard coal based on specific considerations e.g., the geographical origin of the feed coal. The third option allows the user to provide the data for the feed coal. The subroutines READIN and FBED1D were also modified to accommodate the coal input data for the devolatilization submodel. The devolatilization submodel data for all the coals to be used in the final simulations, based on the first option were prepared and submitted to AFR for their review and final approval. AFR approved the devolatilization submodel data to be used in conjunction with FG-DVC.

FBED-1 Code Development

The modifications in the FBED-1 code to improve the model predictions were continued. New improved expressions to calculate the internally consistent coal/char and gas phase enthalpies were derived and a new procedure to simulate the energy exchange effects between the solid and the gas phases during devolatilization was incorporated into the code. A new subroutine, HDEVOL, was written to calculate the heat release rate during devolatilization. The new algorithm is based on the model proposed by Merrick (1983). The Merrick's model, which considers nine species including tar, was extended to accommodate twenty seven functional groups of the FG-DVC devolatilization submodel. Figure III.B-1 shows the results of the simulations made with the previous and the new formulations. Figure III.B-1A shows the steep temperature gradient during devolatilization which is caused by heat exchange effects due to high devolatilization rates as shown in Figure III.B-1B. The simulations made with the new submodel show reasonable temperature gradients for the solid during devolatilization as shown in Figure III.B-1C. The sharp devolatilization spike observed during the previous simulations is eliminated, and with the new submodel devolatilization is not very localized (Fig. III-B.1D). The tar evolution from the first mass bin, with the lowest effective molecular weight, still showed some unstable behavior. This problem was brought to the attention of AFR.

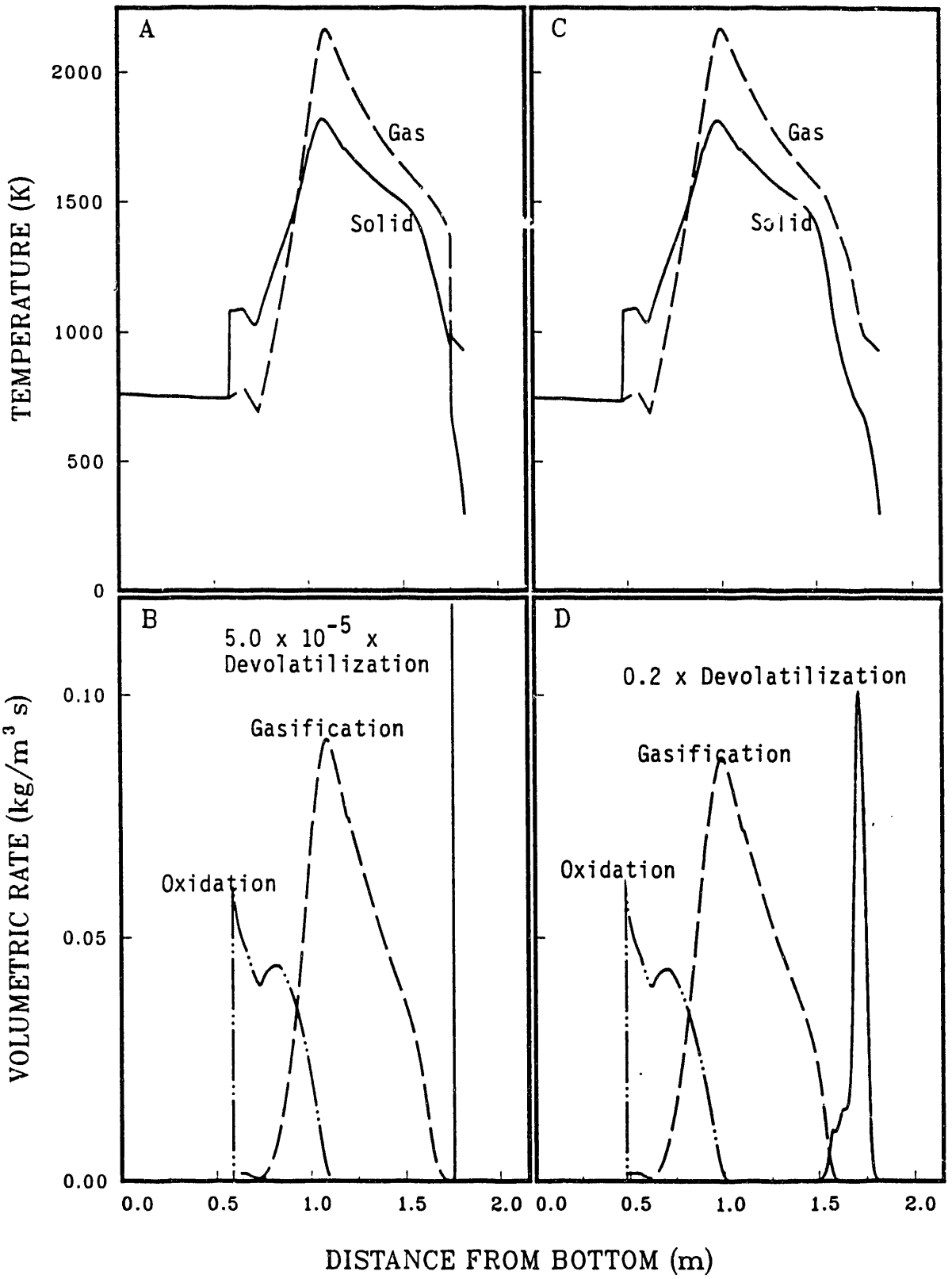

Figure III.B-1. Comparison of temperature and volumetric rate profiles: A) temperature profiles with the old devolatilization energy exchange formulation, B) volumetric rate profiles with the old devolatilization energy exchange formulation, C) temperature profiles with the new devolatilization energy exchange formulation, D) volumetric rate profiles with the new devolatilization energy exchange formulation.

The fixed-bed model was also extended to account for the decomposition of tar in the gas phase. A new subroutine, TCRACK, was added to the FBED-1 code. The tar cracking submodel is based on the following assumptions: 1) the ith functional group in tar evolves to the ith functional group in gas, 2) the decomposition of tar follows the same kinetics as that of gas evolution from the char, and 3) the evolution of gas from tar takes place at the gas temperature. The kinetic rates for the gas phase decomposition of tar may be determined either with variable or fixed Gaussians. The code was executed successfully when rates are computed with a variable gaussian. The system of equations becomes extremely stiff when the kinetic rates were computed using a fixed gaussian, and with this option the code, as yet, has not been executed successfully.

The study of the zero-dimensional part of the code to yield better estimates for the one-dimensional portion was initiated. The option to allow the thermal decomposition of the tar in the gas phase of the drying and devolatilization zone was added. The gas phase thermal decomposition of the recycle tar in the equilibrium zone of the zero-dimensional model was also added. The comparison of the predicted and the experimental results with these options is yet to be made. The submodel to calculate the gas phase equilibrium properties is being studied to allow the inclusion of a pure condensed (solid) phase in the equilibrium calculations.

The FBED-1 code was further modified to provide the options for using a simpler devolatilization submodel, FG-SET. The integration of the FG-SET submodel, with either twenty seven or nineteen functional groups, required major changes in some subroutines as: 1) the number of equations in the system is reduced and 2) the potential tar forming fraction, x0, is either user specified or computed using the correlation of Ko et al., (1988), whereas with the FG-DVC submodel it is computed by the DVC portion of the model. The code was modified to use a dynamic array length for the dependent variables vector y. The length of the array y is computed internally based on the options for the devolatilization and the tar decomposition submodels. These modification were made in a way that an addition of more dependent variables in zero-dimensional or one-dimensional portions of the code could be made with minimal efforts. Figures III.B-2 to III.B-4 show the results of simulation with three options: 1) FG-DVC, 2) FG-SET with user specified potential tar forming fraction, x0, and 3) FG-SET with x0 computed using the correlation of Ko et al. The value of the potential tar forming fraction for the FG-SET with

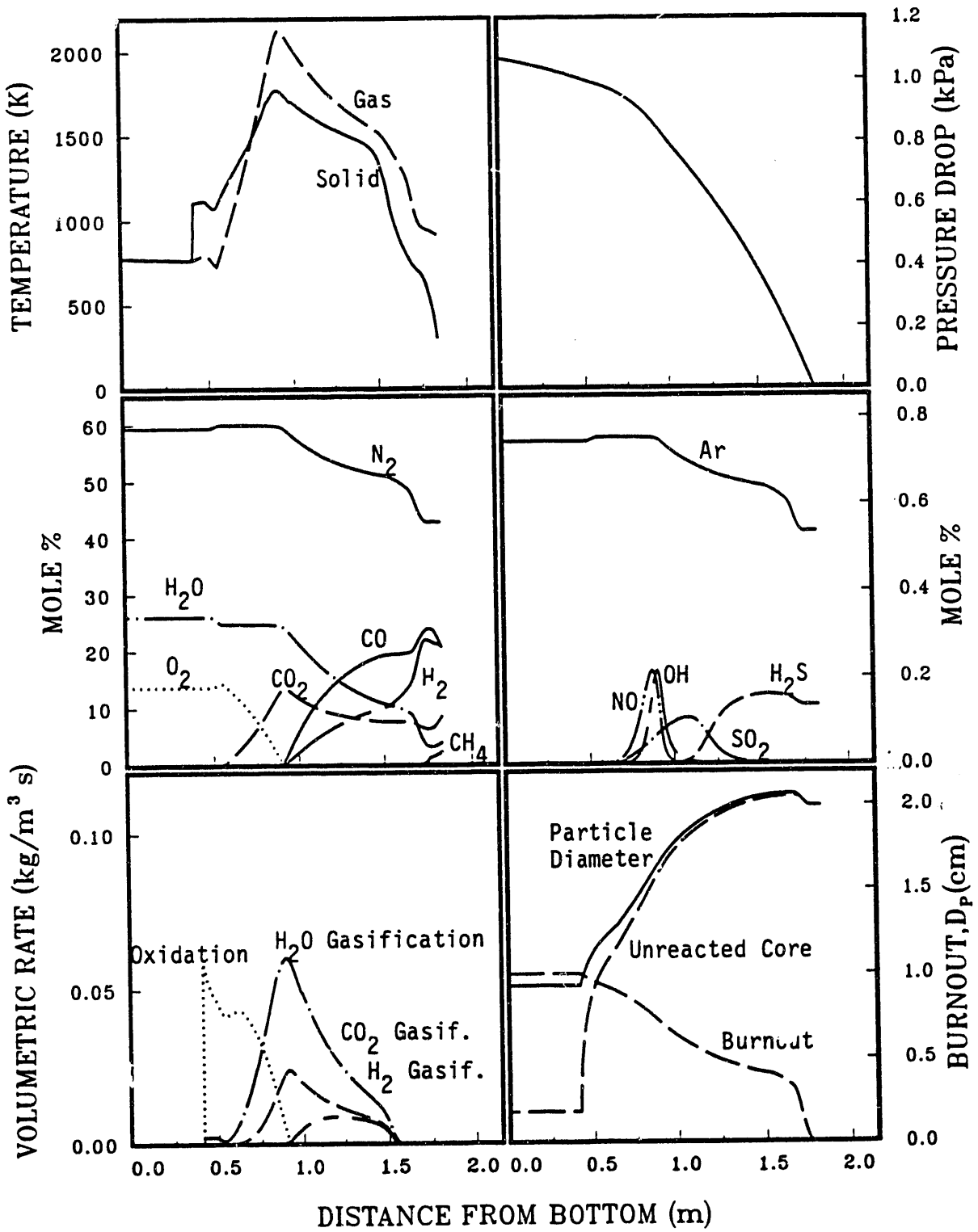

Figure III.B-2. FBED-1 predictions with FG-DVC devolatilization submodel.

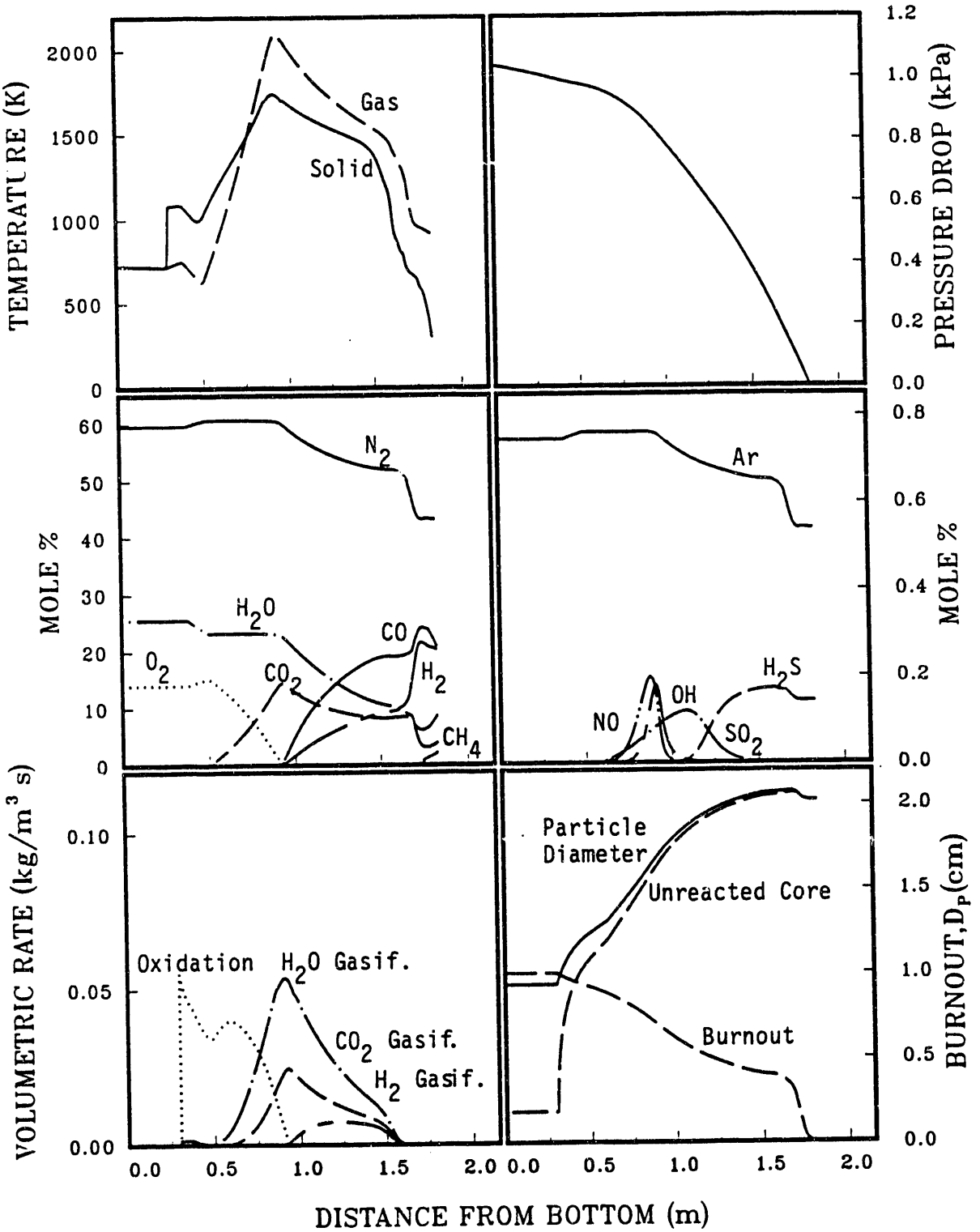

Figure III.B-3. FBED-1 predictions with FG-SET devolatilization submodel, with user specified potential tar forming fraction, (x0=0.153).

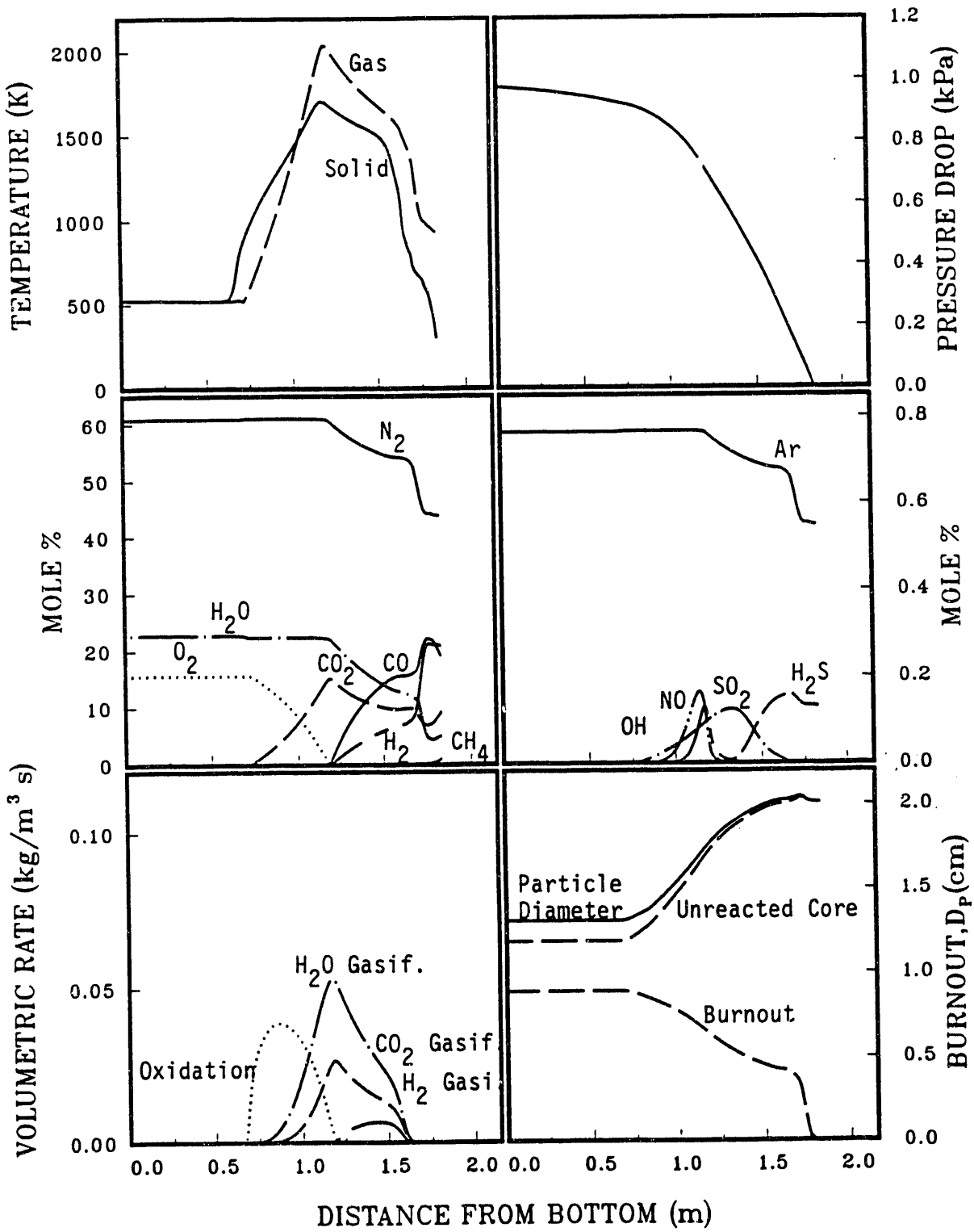

Figure III.B-4. FBED-1 predictions with FG-SET devolatilization submodel, with the potential tar forming fraction computed with Ko's correlation, (x0=0.253).

user specified option was assigned to be 0.153 which was obtained from the zero-dimensional portion of the simulation with FG-DVC option. No significant changes are observed in the profiles except that oxidation zone is comparatively longer and the temperature jumps near the ash zone are more pronounced. The ash zone temperature also decreases by about 50 K. The simulation with FG-SET and xO computed by Ko's correlation shows a strong effect of potential tar-forming fraction. The reaction zone is compressed. The jumps in temperatures near the ash zone are not observed. The temperature at the end of the oxidation zone is also lower by about 200 K. The conversion of char is not complete, as can be seen from the burnout profile. This may be caused by the lower final oxidation zone temperature. The differences are being studied and the efforts are underway to explain them.

The study of the individual subroutines was also continued. Some corrections were made in the sensible enthalpy calculation for the tar. The expressions for the calculations of total enthalpy of tar and char were rewritten as separate functions to eliminate the repetitive code from the various modules and to improve the code structure. The subroutines TRANSP and MTCOEF, which calculate the transports properties of the mixture and the mass transfer coefficients, were rewritten. The calculations for the collision integrals for viscosity and diffusivity were also improved and are now based on the relations of Neufield with Brokaw's correction (1969). Minor corrections were made in the input data for the Stockmayer-Potential parameters for the polar compounds e.g., H_2O. The modified subroutines were tested and the results were compared with the literature values. The integration of these modules in the code was completed.

The operating systems on both Sun 4/330 and SPARC station 1 were updated to Sun OS 4.1.1. The new operating system includes the Openwindows software which is to be used for the graphical output of the fixed-bed code. The generic versions of the DISSPLA graphics programs were completed to be used for the final version of FBED-1.

Plans

During the next quarter, the comprehensive fixed-bed model, FBED-1, will be completed. Axial heat and mass transfer effects will be added. A procedure for alternating integration from the top and from the bottom of the gasifier will be implemented. The iteration method will be further modified

to improve the convergence and the robustness of the code. After completion, the code will be validated and a sensitivity analysis will be performed. Work will be completed to support spreadsheet graphics on Macintosh as well as DISSPLA graphics on SUN and Silicon Graphics. Preparation of the FBED-1 user's manual will be completed. The code will be delivered to and installed at METC.

SUBTASK 3.C. - GENERALIZED FUELS FEEDSTOCK SUBMODEL

Senior Investigators - B. Scott Brewster and L. Douglas Smoot
Brigham Young University
Provo, UT 84602
(801) 378-6240 and 4326

Objective

The objective of this subtask is to generalize PCGC-2 to include sorbent injection, as outlined in the Phase II Research Plan.

Accomplishments

Simulation of the BYU gasifier with and without sidewall injection of sorbent was completed. The cases that were simulated are Test No. I9, Sample No. 3 (without sorbent injection) and Test No. I10, Sample No. 4 (with sorbent injection) from Table II.H-2 in the 3rd Annual Report (Solomon et al., 1989). As discussed under Subtask 2.g, the results are presented in a paper that is included in the appendix. As previously mentioned, the degree of sulfur capture was over-predicted, presumably because of inadequate representation of the 3-D mixing effects due to sidewall injection. Thus, while generalized feeding of solids (e.g. sorbent) in sidewall inlets has been accomplished in the code, the applicability of the code to such configurations appears to be limited. Better predictions with the 2-D code are expected when the feed geometry in the physical apparatus is truly axisymmetric.

Plans

The testing of the sorbent injection submodel is now complete. No further work is planned on this subtask.

SECTION IV. TASK 4. APPLICATION OF INTEGRATED CODES

Objective

The objectives of this task are to evaluate the integrated comprehensive codes for pulverized coal and fixed-bed reactors and to apply the codes to selected cases of interest to METC.

Task Outline

This task will be accomplished in two subtasks, one for the entrained-bed lasting 57 months and one for the fixed-bed lasting 48 months. Each of these subtasks will consist of three components: 1) Simulation of demonstration cases on BYU computers; 2) Implementation on a work station at AFR; and 3) Simulations of demonstration cases on the workstation.

IV.A. SUBTASK 4.A. - APPLICATION OF GENERALIZED, PULVERIZED-COAL COMPREHENSIVE CODE

Senior Investigators - B. Scott Brewster and L. Douglas Smoot
Brigham Young University
Provo, UT 84602
(801) 378-6240 and 4326

Research Assistant - Ziaul Huque

Objectives

The objectives of this subtask are to 1) demonstrate application of the code by simulating reactors of interest to METC and 2) implement the code at METC and conduct training.

Accomplishments

One of the two application cases, namely, the Coal Tech cyclone combustor (a Clean Coal Technology project) has been simulated with the updated version of the FG-DVC submodel in PCGC-2. A schematic diagram of the horizontally-fired reactor is shown in Figure IV.A-1 (Zauderer and Fleming, 1991). Primary and secondary streams consist of air. Coal and sorbent particles are injected through an additional inlet located on the side wall, with air as the carrier gas. Pulverized coal, air and sorbent are injected toward the wall to cause cyclonic action. The secondary gas is injected with an inlet swirl. The air and coal flow rates are that of Case 132 given in the U.S. DOE Clean Coal Program Final Report (Zauderer and Fleming, 1991). Sorbent injection and sulfur capture calculations were not carried out at this stage.

All the dimensions are normalized by the length and diameter of the reactor such that they vary from 0 to 1. Results of the preliminary simulations are presented in this report. Figure IV.A-2 shows the plot of velocity vectors along with particle trajectories. The plot shows two isolated recirculation zones. Some of the particles are thrown against the side wall where they are assumed to stick and continue burning. Complete burnout of coal was obtained close to the exit, at a normalized axial distance of about 0.77 as shown in Figure IV.A-3. Figure IV.A-4 shows the trajectory

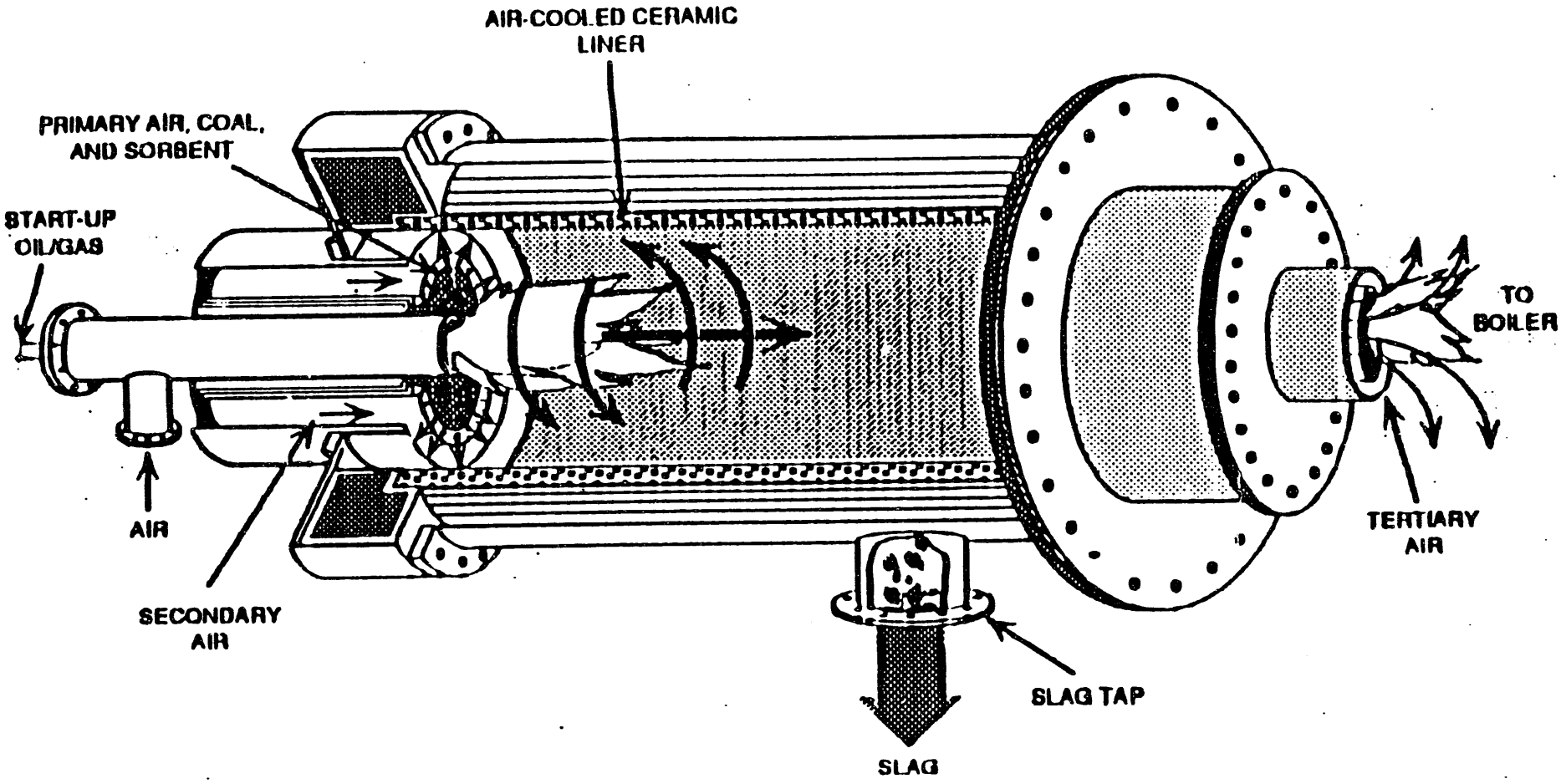

Figure IV.A-1. Schematic of Coal Tech cyclone combustor [Zauderer B., et al., 1991].

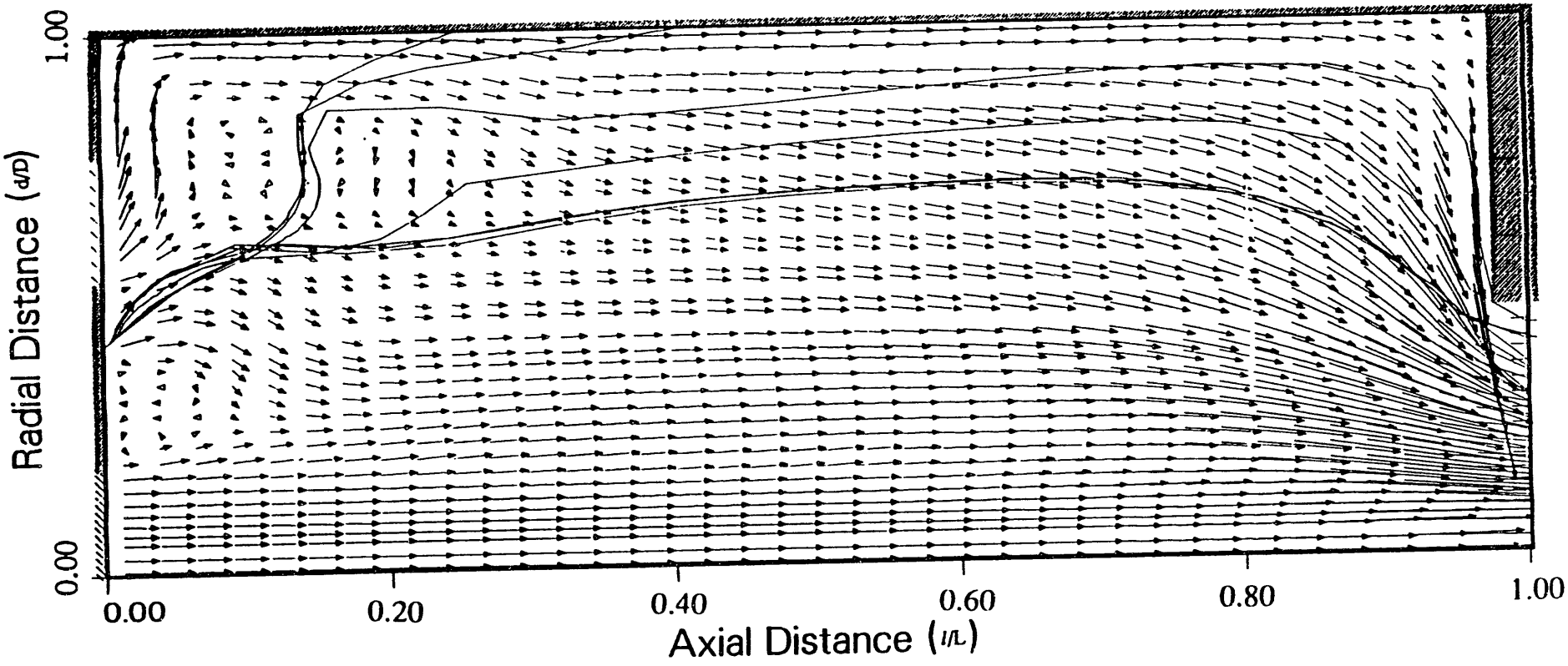

Figure IV.A-2 Two-dimensional velocity vectors and particle trajectories predicted for Coal Tech cyclone combustor.

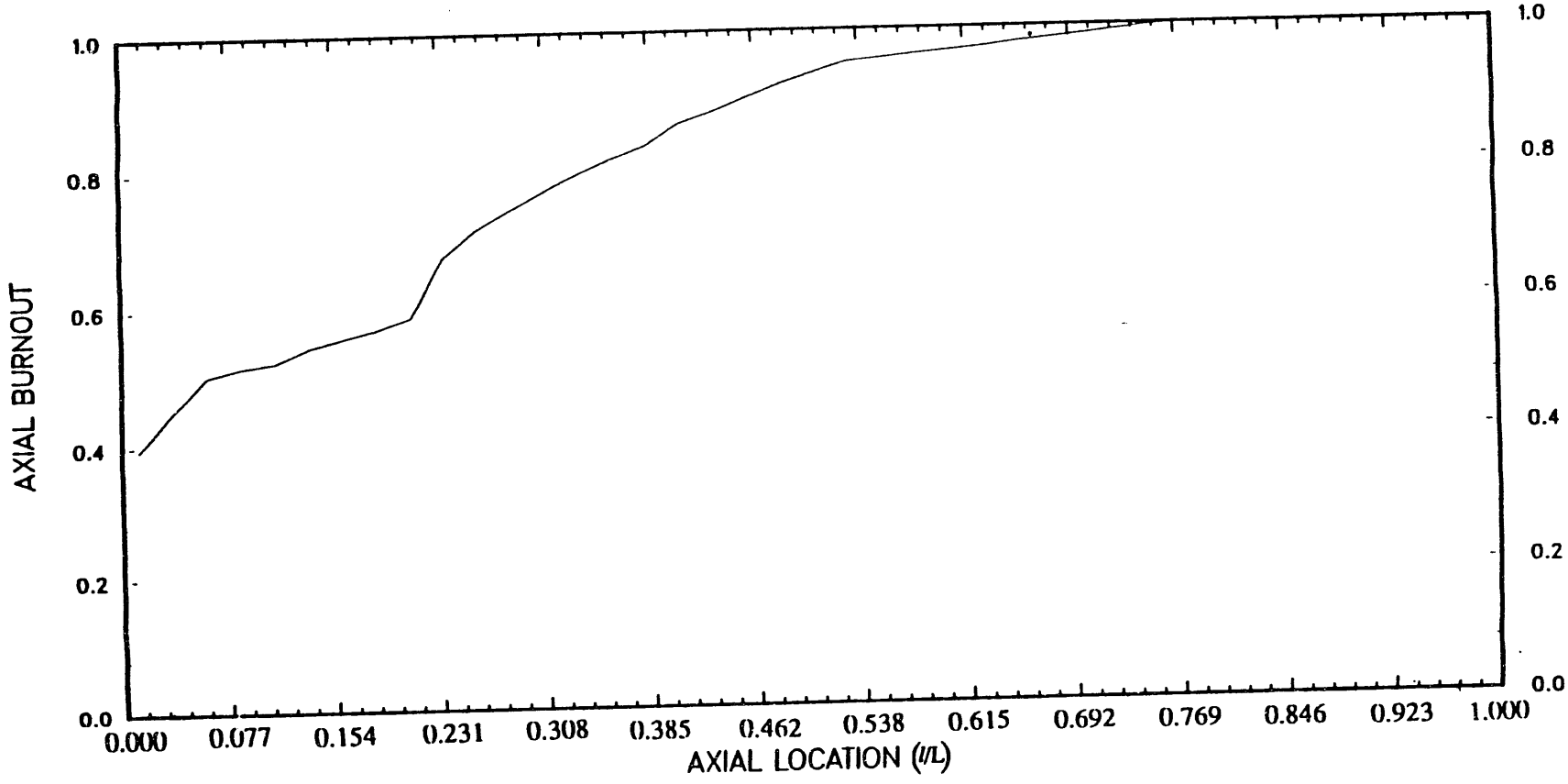

Figure IV.A-3. Radially averaged axial burnout predicted for Coal Tech cyclone combustor.

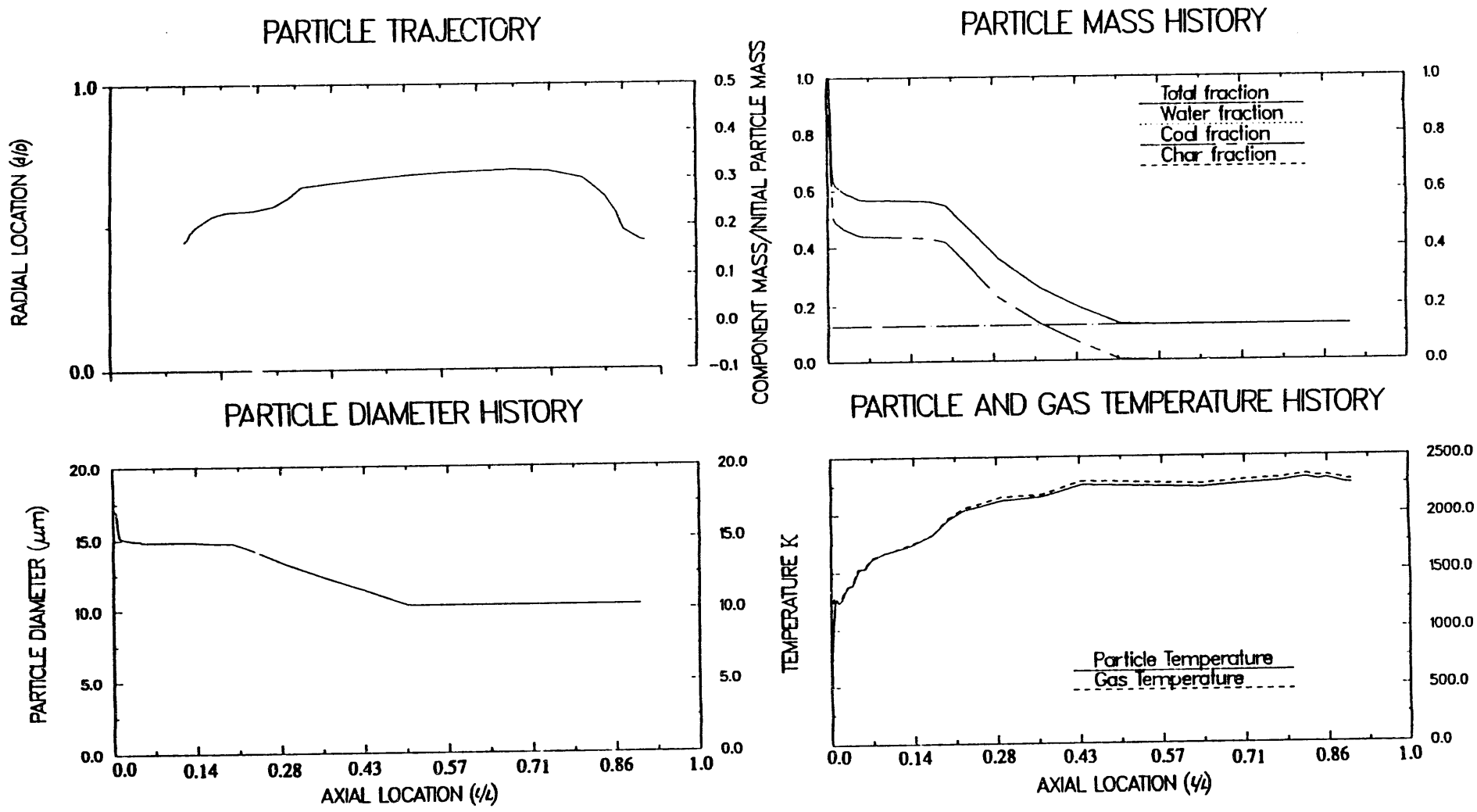

Figure IV.A-4. Trajectory, mass, diameter and temperature history predicted for 17 mm size particle for Coal Tech cyclone combustor.

and mass, diameter and temperature of particles of size 17 mm. Burnout for this particle size was complete at a normalized axial location of about 0.5. Temperature reached a maximum value of about 2250 K.

Plans

Complete application cases and prepare final report.

IV.B. SUBTASK 4.B. - APPLICATION OF FIXED-BED CODE

Senior Investigators - Predrag T. Radulovic and L. Douglas Smoot
Brigham Young University
Provo, Utah 84602
(801) 378-3097 and (801)378-4326

Research Assistant - M. Usman Ghani

Objectives

The objective of this subtask is to apply the advanced fixed-bed code developed in task 3.b. to simulate fixed bed gasifiers of interest to METC.

Accomplishments

Fixed-Bed Data Collection

During the past quarter, work continued on collecting fixed-bed design and test data from organizations and individuals involved in fixed- or moving-bed gasification or combustion research or in research on non-reacting fixed- or moving beds. No new data sets were obtained. Work also continued on collecting fixed-bed experimental data from the open literature.

Application of Fixed-Bed Code

No new cases were simulated.

Plans

During the next quarter, work will be completed on collecting fixed-bed design and test data. The code will be applied to the cases of interest to METC.

REFERENCES

Brokaw,R.S., Ind. Eng. Chem. Process Design Develop., 8, 240, (1969).

Coburn,T.T., Foster, K.G., Gregg, H.R., and Lindsey, J.A., Tests of a Mechanism for H_2S Release During Coal Pyrolysis, Intl. Conf. of Coal Science, 616, Science Press, (1991).

Crowe,C.T., Sharma, M.P. and Stock, D.E., "The particle-source-in-cell (PSI-CELL) model for gas-droplet flows," J. Fluids Eng., Trans. of the ASME, 99, 325-332 (1977).

Dryden, I.G.C., and Sparham, G.A., "Carbonization of Coals Under Gas Pressure", B.C.U.R.A. Monthly Bull., 27, 1 (1963).

Hobbs,M.L., Radulovic, P.T., and Smoot, L.D., "Modeling Fixed-Bed Coal Gasifiers,"AIChE J., 38, 681 (1992).

Khan, M. Rashid, Presiction of Sulfur Distribution in Products During Low Temerature Coal Pyrolysis and Gasification, Fuel, 68, 1439, (1989).

Keleman,S.R., Gorbaty, M.L., Vaughn, S.N., and George G., ACS Div. of Fuel Chem. Prepr., Vol 36 (3), 1225 (1991).

Ko, G.H., Sanchez, D. M., Peters, W. A., and Howard, J. B., "Correlations for Effects of Coal Type and Pressure on Tar Yields from Rapid Devolatilization," *Twenty-Second Symposium (International) on Combustion*, The combustion Institute, Pittsburgh, PA, 115, (1988).

Merrick,D., "Mathematical models of the thermal decomposition of coal 2. Specific heats and heats of reactions," *Fuel*, 62, 540, (1983).

Nicoletti, P.A., METCEC - USER'S MANUAL, Final Report, DOE-METC Contract No. DE-AC21-85MC21353, EG&G WASC, Inc., Morgantown, WV, (1986a).

Nicoletti, P.A., METCEC - PROGRAM LOGIC MANUAL, Final Report, DOE-METC Contract No.DE-AC21-85MC21353, EG&G WASC, Inc., Morgantown, WV, (1986b).

Silcox, G.D., "Analysis of the SO2-lime reaction system: Mathematical modeling and experimental studies emphasis on stoker applications," Ph.D. dissertation, The University of Utah, (1985).

Silcox, J.D., Kramlich, J.C. and Pershing, D.W., "The mathematical modeling for the flash calcination of dispersed CaCO3 and Ca(OH)2 particles," Ind. Eng. Chem., 28, 155 (1989).

Solomon, P.R., Serio, M.A., Hamblen, D.G., Smoot, L.D. and Brewster, B.S., Measurement and modeling of advanced coal conversion processes, 22nd Quarterly Report, DOE-METC Contract No. DE-AC21-86MC23075, Advanced Fuel Research, Hartford, CT, (1992).

Solomon, P.R., Serio, M.A., Hamblen, D.G., Smoot, L.D. and Brewster, B.S., Measurement and modeling of advanced coal conversion processes, 21st Quarterly Report, DOE-METC Contract No. DE-AC21-86MC23075, Advanced Fuel Research, Hartford, CT, (1991).

Solomon, P.R., Serio, M.A., Hamblen, D.G., Smoot, L.D. and Brewster, B.S., Measurement and modeling of advanced coal conversion processes, 5th Annual Report, DOE-METC Contract No. DE-AC21-86MC23075, Advanced Fuel Research, Hartford, CT, (1991).

Solomon, P.R., Serio, M.A., Hamblen, D.G., Smoot, L.D. and Brewster, B.S., Measurement and modeling of advanced coal conversion processes, 3rd Annual Report, DOE-METC Contract No. DE-AC21-86MC23075, Advanced Fuel Research, Hartford, CT, (1989).

Su, J.L., Perlmutter, D.D., AIChE J., 31, 973, (1985).

Tseng, H.P., Edgar, T.F., Fuel, 63, 385, (1984).

Tseng, H.P., Edgar, T.F., Fuel, 64, 373, (1985).

Vorres, K.S., Energy & Fuels, 4, 420 (1990).

Zauderer, B. and Fleming, E.S., "The demonstration of an advanced cyclone coal combustor, with internal sulfur, nitrogen, and ash control for the conversion of a 23 MMBtu/hour oil fired boiler to pulverized coal," U.S. DOE-Clean Coal Program, Final Technical Report, DOE Cooperative Agreement No. DE-FC22-87PC79799, (1991).

END

DATE FILMED

2/2/93